Aeolian Research 32 (2018) 228–245

Contents lists available at ScienceDirect

Aeolian Research

journal homepage: www.elsevier.com/locate/aeolia

The response of source-bordering aeolian dunefields to sediment-supply changes 1: Effects of wind variability and river-valley morphodynamics☆

Joel B. Sankey[a,*], Alan Kasprak[a], Joshua Caster[a], Amy E. East[b], Helen C. Fairley[a]

[a] Grand Canyon Monitoring and Research Center, Southwest Biological Science Center, U.S. Geological Survey, Flagstaff, AZ, USA
[b] Pacific Coastal and Marine Science Center, U.S. Geological Survey, Santa Cruz, CA, USA

ARTICLE INFO

Keywords:
Change detection
Aeolian dune
Dam
Fluvial
Modelling
River regulation

ABSTRACT

Source-bordering dunefields (SBDs), which are primarily built and maintained with river-derived sediment, are found in many large river valleys and are currently impacted by changes in sediment supply due to climate change, land use changes, and river regulation. Despite their importance, a physically based, applied approach for quantifying the response of SBDs to changes in sediment supply does not exist. To address this knowledge gap, here we develop an approach for quantifying the geomorphic responses to sediment-supply alteration based on the interpretation of dunefield morphodynamics from geomorphic change detection and wind characteristics. We use the approach to test hypotheses about the response of individual dunefields to variability in sediment supply at three SBDs along the Colorado River in Grand Canyon, Arizona, USA during the 11 years between 2002 and 2013 when several river floods rebuilt some river sandbars and channel margin deposits that serve as sediment source areas for the SBDs. We demonstrate that resupply of fluvially sourced aeolian sediment occurred at one of the SBDs, but not at the other two, and attribute this differential response to site-specific variability in geomorphology, wind, and sediment source areas. The approach we present is applied in a companion study to shorter time periods with high-resolution topographic data that bracket individual floods in order to infer the resupply of fluvially sourced aeolian sediment to SBDs by managed river flows. Such an applied methodology could also be useful for measuring sediment connectivity and anthropogenic alterations of connectivity in other coupled fluvial-aeolian environments.

1. Introduction

Source-bordering aeolian dunefields (SBDs) occur in landscapes around the world where dunes are supplied with sediment from upwind deposits originally emplaced by water (Bullard and McTainsh, 2003; May, 2014). Examples include coasts where marine sand supplies inland aeolian dunes (Nordstrom and Jackson, 1992; Sherman and Lyons, 1994; Psuty, 1996; Marqués et al., 2001; Hesp, 2002; Hesp et al., 2005, Bauer et al., 2009; Houser, 2009; Houser and Mathew, 2011), lacustrine environments where sandy shorelines supply aeolian dunes on lake margins (Wopfner and Twidale, 1988; Davidson-Arnott and Law, 1990; Kocurek and Lancaster, 1999; Gillette et al., 2001; Reheis et al., 2002; Wiggs et al., 2003; Yu et al., 2013), and river valleys where fluvial sediment supplies aeolian deposits adjacent to the floodplain (Page, 1971; Page et al., 2001; Ivester and Leigh, 2003; Rendell et al., 2003; Han et al., 2007; Draut, 2012; Muhs et al., 2013; Al-Masrahy and Mountney, 2015; Bogle et al., 2015). SBDs that are primarily built and maintained with river-derived sediment are found in many large river valleys around the world (Liu and Couthard, 2015). SBDs in river valleys are scientifically and societally relevant because they can preserve important paleoenvironmental information and archaeological evidence of past human activity and occupation (Vanderwal, 1978; Ivester and Leigh, 2003; Draut et al., 2008; Pederson and O'Brien, 2014; Roskin et al., 2014; East et al., 2016; Lu et al., 2017). Landscape evolution in SBDs also has important links to ecological processes, as sediment-starved dunes may begin to stabilize with biologic crusts in dryland settings, and this stabilization then promotes further colonization by vegetation communities (Harper and Belnap, 2001; Belnap, 2012; Draut, 2012). Many SBDs, and specifically the sediment supply on which they depend, are currently impacted by changes in climate, land use, and modification of river flows and sediment availability (Fryberger and Dean, 1979; Davidson-Arnott and Law, 1990; Draut, 2012; Al-Masrahy and Mountney, 2015; East et al., 2016). Therefore, quantifying the geomorphic response to those forcings is key to understanding how aeolian landscapes are, and will be, affected by changing climate, land use, and river regulation.

River regulation refers to the management of flows via dams for hydropower, flood control, water storage or diversion for

DOI of original article: http://dx.doi.org/10.1016/j.aeolia.2018.02.004
☆ Note that this manuscript is a companion to [Aeolian Research 32 (2018) 154–169] in this issue.
* Corresponding author at: Grand Canyon Monitoring and Research Center, Southwest Biological Science Center, U.S. Geological Survey, Flagstaff, AZ 86001, USA.
E-mail address: jsankey@usgs.gov (J.B. Sankey).

https://doi.org/10.1016/j.aeolia.2018.02.005
Received 31 October 2017; Received in revised form 16 February 2018; Accepted 19 February 2018
Available online 06 April 2018
1875-9637/ Published by Elsevier B.V.

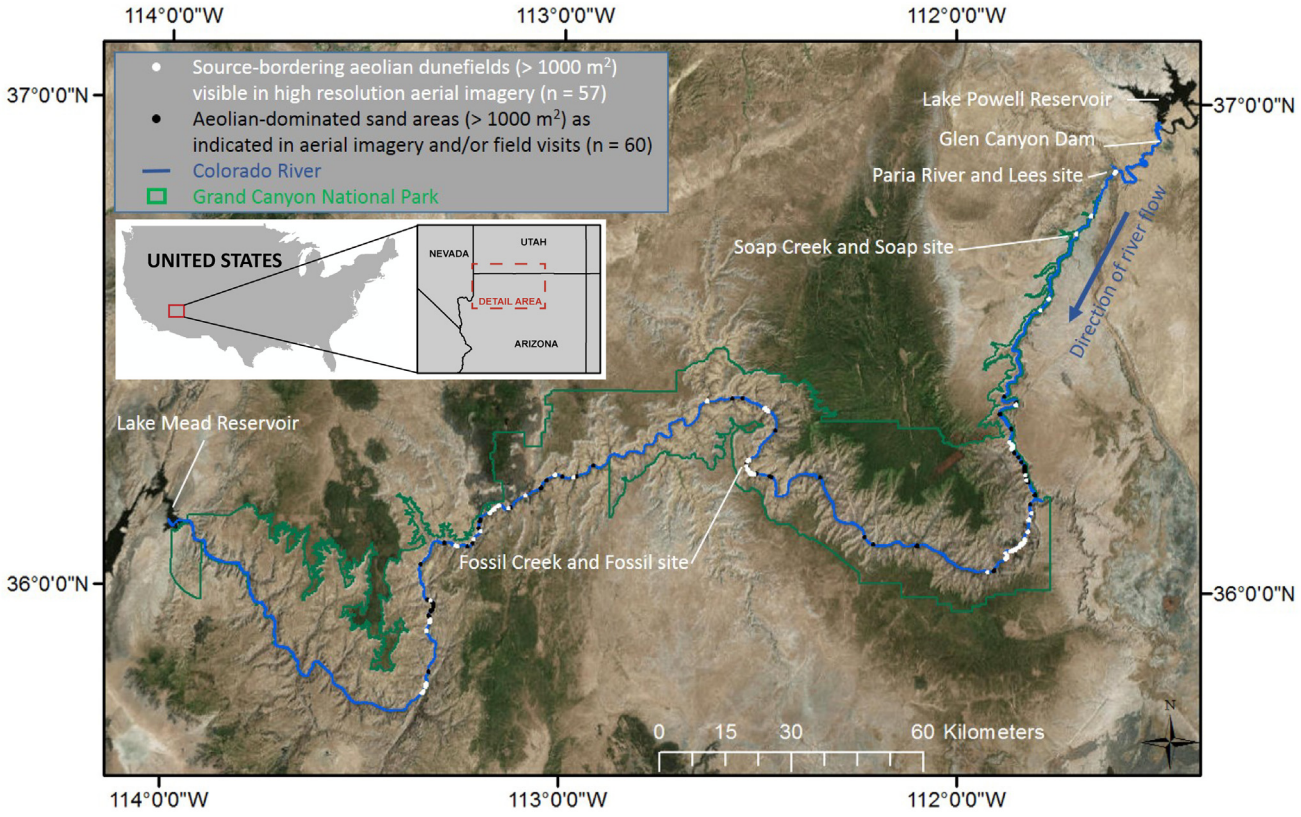

Fig. 1. Map showing locations of the three source-bordering aeolian dunefield (SBDs) study sites, as well as all other large SBDs and other aeolian-dominated sand areas (ADAs) along the Colorado River downstream of Glen Canyon Dam in the Grand Canyon region, Arizona, USA. Grand Canyon National Park extends from the confluence of the Paria and Colorado Rivers to the upstream end of Lake Mead Reservoir. There are currently at least 57 SBDs along the Colorado River in Grand Canyon that are large (spatially contiguous areas of unvegetated sand > 1000 m^2) and have dune morphology that is visible in high resolution aerial imagery. There are another at least 60 ADAs at which aeolian processes are a primary geomorphic process and dune morphology is not visible in aerial imagery but other indicators of aeolian sand transport such as coppice or shadow dunes in the lee of shrubs, boulders, or arroyo channels have either been identified in the field (East et al., 2016) or are visible in aerial imagery.

municipalities, agriculture or industry (Nilsson and Berggren, 2000; Nilsson et al., 2005). Draut (2012) articulated ways in which river regulation, relative to other factors like climate and land use, can affect SBDs in river valleys. Specifically, dams that trap sediment in upstream reservoirs can greatly reduce fluvial sediment supply to the downstream river valley, in turn partially or totally disconnecting SBDs from their former sediment sources. Those sediment-source areas commonly consist of fluvial sandbars that are unvegetated or sparsely vegetated, and that are dry for sufficient time to allow aeolian sand entrainment and transport. The decrease in aeolian sediment supply when those fluvial sand sources are depleted in a dam-controlled river can ultimately lead to erosion, or reduction in aeolian activity that may lead to dune stabilization by vegetation colonization, within SBDs that were formed and maintained with fluvial sediment prior to river regulation.

The Colorado River in the Grand Canyon region, USA, downstream of Glen Canyon Dam, is an example of a river valley where SBDs are common (Figs. 1 and 2) and have been dramatically impacted by river regulation (Draut, 2012). This segment of the river is deprived of sediment by the dam, which is approximately 24 km upstream of Grand Canyon National Park and effectively reduces the downstream sediment supply by 85–95% from pre-dam levels (Topping et al., 2000; Rubin et al., 2002; Wright et al., 2005). Operations of the dam for hydropower generation since 1963 have fundamentally altered the flow regime of the Colorado River in Grand Canyon, and have largely eliminated pre-dam low flows that historically exposed large areas of subaerial bare sand (Kasprak, A., et al., U.S. Geological Survey, Unpublished results). Dam operations have also eliminated large, regularly occurring, sediment-rich spring floods. Moreover, the combination of elevated low flows and elimination of most floods since 1963 has led to widespread riparian vegetation encroachment, further reducing the extent of subaerial bare sand (Sankey et al., 2015). These changes in hydrology, sediment, and riparian vegetation have reduced or eliminated the modern aeolian sediment supply to SBDs (Draut, 2012; East, et al., 2016), thus disconnecting many SBDs from their upwind fluvial sand source areas (e.g., river sandbars). Research into SBD dynamics in Grand Canyon has identified two distinct SBD classes within the Colorado River (Draut and Rubin, 2008; Draut, 2012): those with modern (i.e., post-dam) or relict (i.e., only pre-dam or early post-dam) fluvial sediment supply due to river regulation. Those designations were later refined to include gradations of sediment-supply potential given the local presence of vegetation or topographic barriers between fluvial sand sources and downwind SBDs (East et al., 2016). Several related studies have examined how deposition of fluvially sourced aeolian sediment occurs relative to, and interacts with, processes such as sheetwash, gully erosion, and wind erosion at individual SBDs and other river valley landforms in Grand Canyon (Sankey and Draut, 2014; Collins et al., 2016; East et al., 2016; Kasprak et al., 2017).

In this study we develop and test an analytical framework for the response of individual SBDs to variability in sediment supply caused by river valley morphodynamics and wind. Fig. 3 conceptually illustrates how the response of SBDs to changes in sediment supply should differ for idealized (endmember) unimodal vs. bimodal wind direction regimes. Under a unimodal wind regime with abundant external sediment supply, such as an SBD with modern fluvial sediment supply in Grand Canyon (e.g., Fig. 2A), a dunefield is subject to net sediment import, aeolian deposition, and net aggradation through time. Under a unimodal wind regime with no external sediment supply, such as an SBD with a relict fluvial sediment supply in Grand Canyon (e.g., Fig. 2B), a

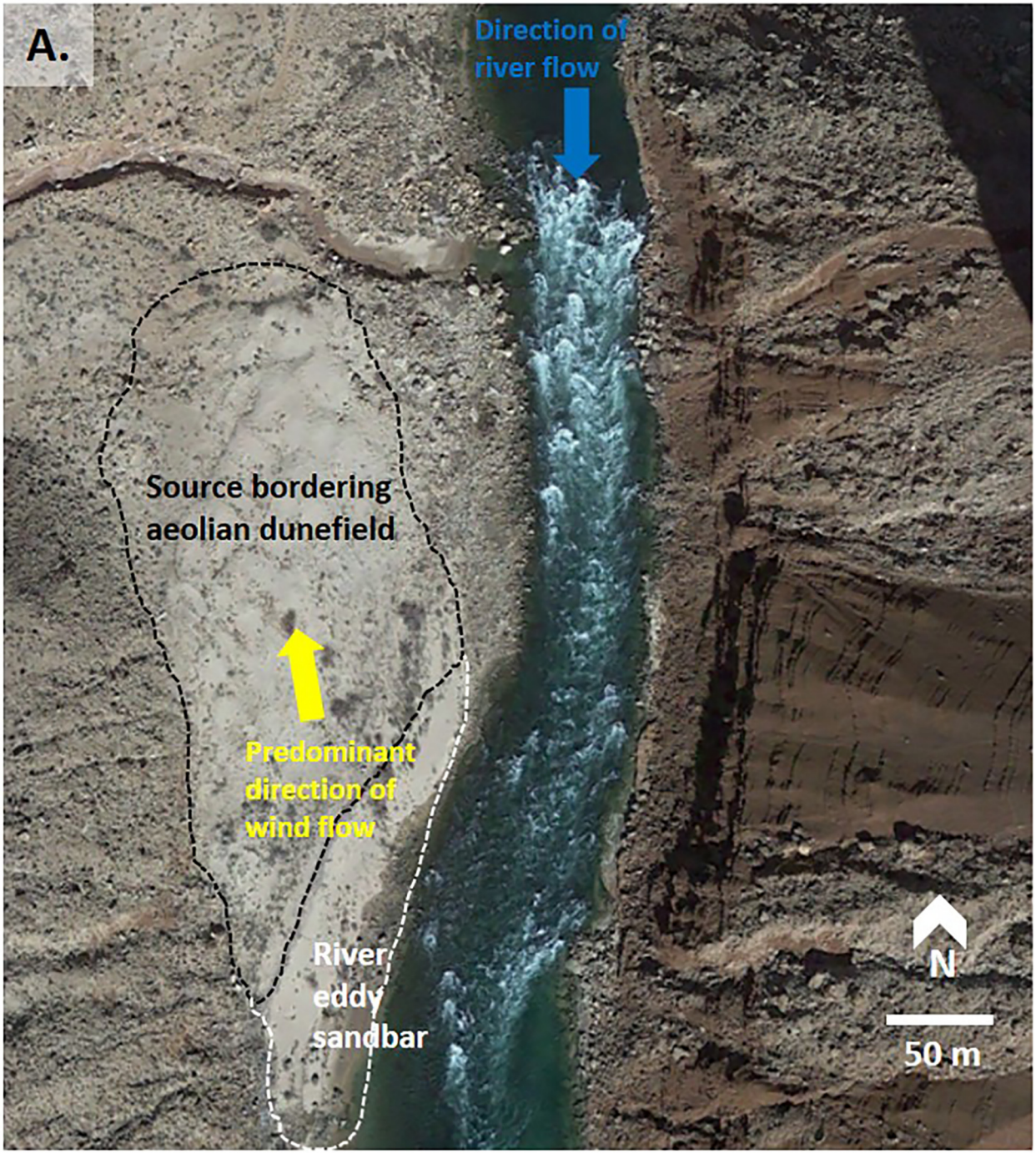

Fig. 2. Annotated aerial images of three source-bordering aeolian dunefields along the Colorado River in Grand Canyon, with differing geomorphic settings relative to wind and river sediment supply. Images were reproduced from Google Earth (dated 2/14/2015 for A, 4/6/2015 for B, and 5/19/2014 for C). A) "Soap" is at the confluence of Soap Creek with the Colorado River and is classified as an SBD with modern fluvial sediment supply; B) "Lees" is at the confluence of the Paria River with the Colorado River and is classified as an SBD with a relict fluvial sediment supply (Draut, 2012). C) "Fossil" is at the confluence of Fossil Creek with the Colorado River and is classified as an SBD with a modern fluvial sediment supply (Draut, 2012). Each SBD is superimposed on other topography such as debris fans that form at the confluence of tributary channels with the river. Tributary confluences and debris fans can constrict the mainstem river channel, which results in river sand deposits in channel margins upstream of the constriction, eddy sandbars downstream of the constriction, and along channel margins elsewhere. SBDs form and persist where wind regimes transport sand from river sediment deposits unimodally upstream and inland or downstream and inland, or bimodally in both directions (i.e., where wind carries sand away from rather than into the river). The predominant wind directions shown are based on weather station measurements at Lees and Soap (introduced in Fig. 7) and inferred at Soap from dune orientation, field experience, and other nearby station measurements.

dunefield is subject to net sediment export, aeolian erosion, and net degradation over time. Finally, under an idealized bimodal wind regime with perfectly opposing winds, net dunefield changes may be relatively minor and independent of external sediment supply, owing to the counteractive geomorphic and sediment transport effects of the opposing winds. Obviously, perfectly bimodal wind direction regimes represent an especially idealized endmember case, and SBDs in Grand Canyon with imperfect bimodal wind direction regimes (e.g., Fig. 2C) may undergo morphodynamic evolution based on whether a modern fluvial sediment supply exists and whether the wind regime ultimately

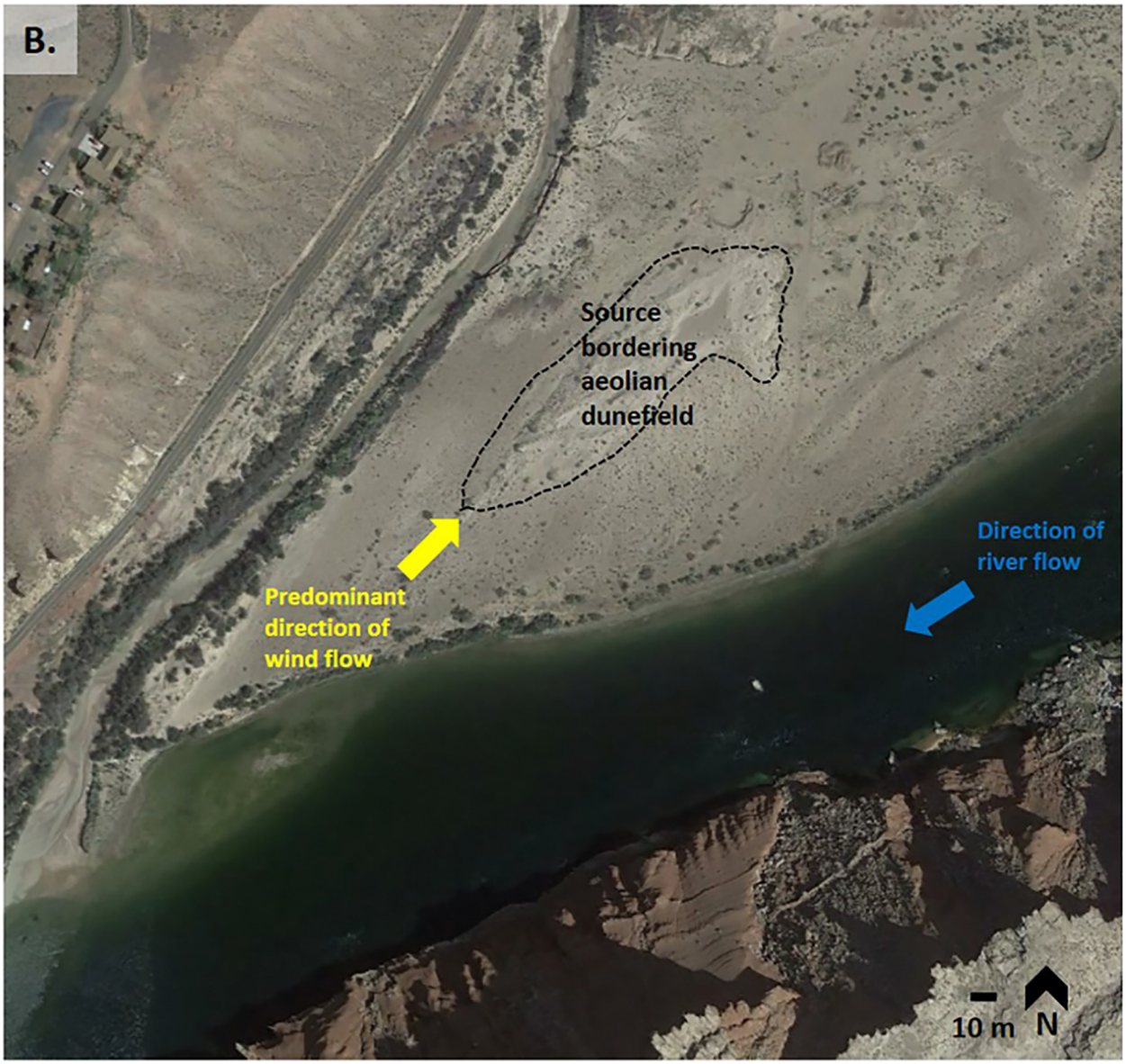

Fig. 2. (*continued*)

transports more sediment towards, instead of away from, the dunefield.

In this study, we first use a Python implementation of the Werner dune model (Barchyn and Hugenholtz, 2012) to illustrate potential morphodynamic responses of simulated SBDs to the endmember scenarios of idealized unimodal and bimodal wind regimes with and without external sediment supply, as illustrated conceptually in Fig. 3. We then use meteorological data, remote-sensing observations, and empirical analyses to test specific hypotheses about the response of individual Grand Canyon SBDs to variability in sediment supply using geomorphic change detection of multi-temporal, high resolution topographic datasets spanning from 2002 to 2013 along the Colorado River in Grand Canyon. We test hypotheses at one SBD ("Soap") with a unimodal wind regime and modern fluvial sediment supply, at a second SBD ("Lees") with a unimodal wind regime and relict fluvial sediment supply, and a third SBD ("Fossil") with bimodal wind regime and modern fluvial sediment supply. Our hypotheses for the observational period from 2002 to 2013 are:

H1. The Soap dunefield, with a presumed unimodal wind regime and modern fluvial sediment supply, will aggrade in the upwind portions of the dunefield, while individual dunes migrate downwind.

H2. The Lees dunefield, with a unimodal wind regime and no modern fluvial sediment supply, will deflate, particularly in the upwind portions of the dunefield, while individual dunes migrate downwind.

H3. The Fossil dunefield, with a multi-modal wind regime and modern fluvial sediment supply, will aggrade in the upwind (based on vector summation) end of the dunefield, but will not show clear evidence of directional migration of individual dunes downwind (based on vector summation).

We anticipate that the results will allow scientists and land managers to better quantify the role of sediment supply and wind conditions in driving aeolian landscape evolution, and to forecast the response of these landscapes to anticipated alterations in sediment supply. In a companion paper to this study (Sankey et al., 2018) we specifically apply the analytical framework to shorter, event-scale time periods with high resolution topographic data that bracket individual controlled floods in order to infer the resupply of fluvially sourced aeolian sediment to SBDs by managed river flows.

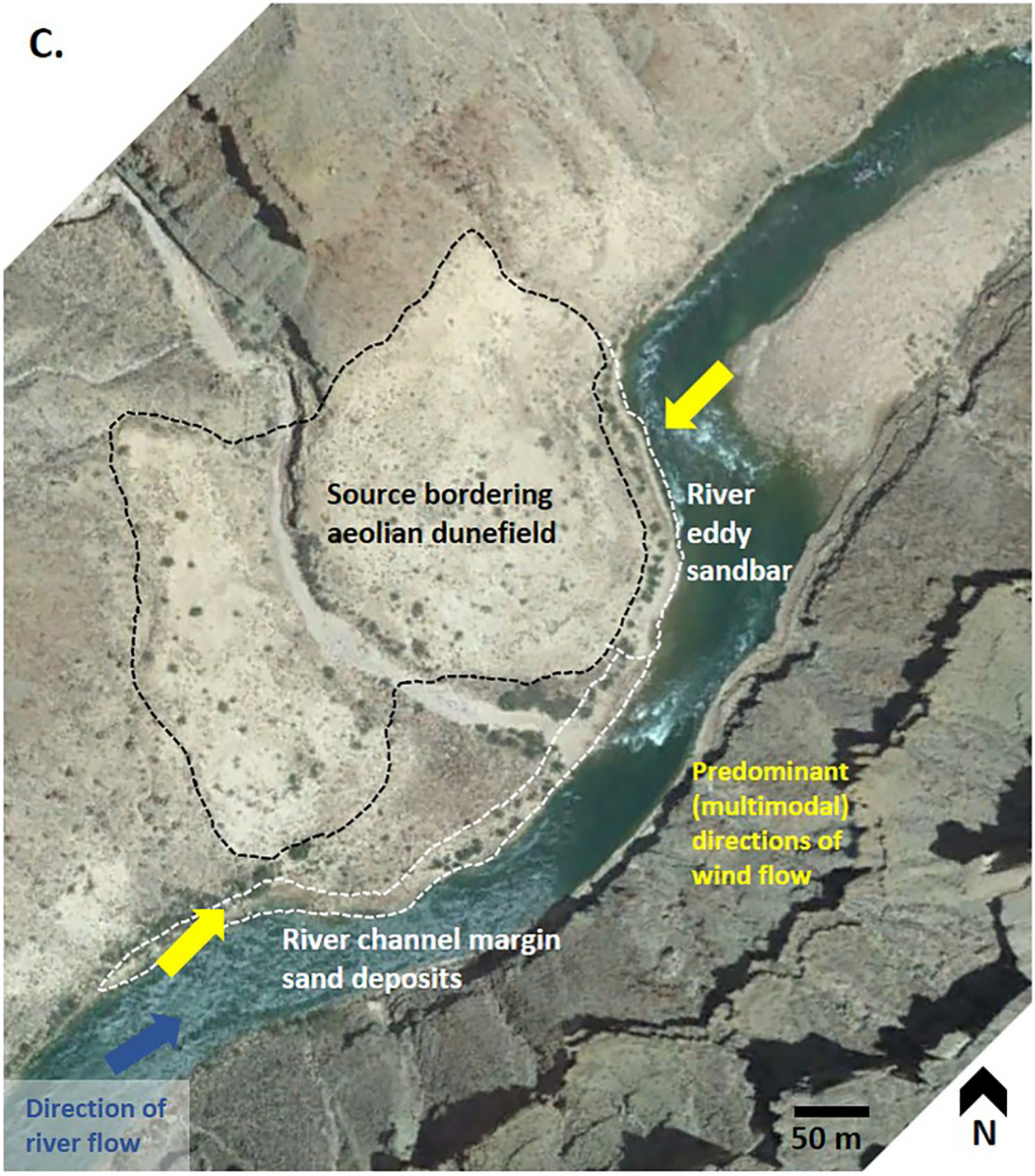

Fig. 2. (*continued*)

2. Data and methods

2.1. Physical setting

Sediment transported by the Colorado River through Grand Canyon is stored on the river bed and in recirculation zones, or eddies, that typically house separation or reattachment sandbars in the lee of debris fans (Schmidt, 1990; Hazel et al., 2006). Alternatively, sandbars can also be found lining pools and channel margins upstream of debris fans (Schmidt, 1990). SBDs commonly occur downwind of present or past locations of sandbars, with aeolian sand overlying topographic features such as debris fans, fluvial terraces, or even as sand ramps deposited atop the base of steep talus slopes. There are currently at least 57 SBDs along the Colorado River in Grand Canyon that are relatively large (spatially contiguous areas of unvegetated sand $> 1000\,m^2$) and have dune morphology that is visible in high-resolution aerial imagery (Fig. 1). There are at least another 60 similarly large areas of unvegetated sand (ADAs; aeolian-dominated areas) at which aeolian processes are a primary mechanism of geomorphic change and although dune morphology is not visible in aerial imagery, other indicators of recent aeolian sand transport (e.g., coppice dunes and shadow dunes in the lee of shrubs, boulders, or arroyo channels) have either been identified in the field (East et al., 2016) or are visible in aerial imagery (Fig. 1). We distinguish SBDs from ADAs because the presence of

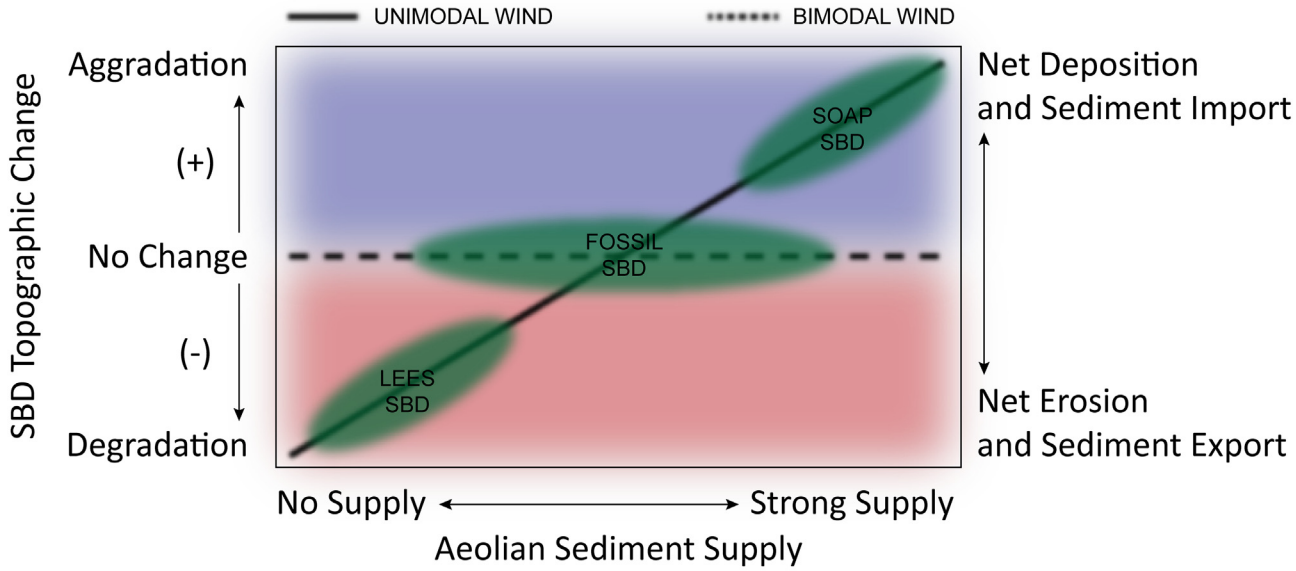

Fig. 3. Conceptual illustration of the differential responses of SBDs to changes in sediment supply for idealized unimodal vs. bimodal wind direction regimes. Under a unimodal wind regime with abundant external sediment supply, such as an SBD with modern fluvial sediment supply in Grand Canyon (e.g., Fig. 2A), a dunefield is subject to net sediment import, aeolian deposition, and net aggradation through time. Under a unimodal wind regime with no external sediment supply, such as an SBD with a relict fluvial sediment supply in Grand Canyon (e.g., Fig. 2B), a dunefield is subject to net sediment export, aeolian erosion, and net degradation over time. Finally, under an idealized bimodal wind regime with perfectly opposing winds, net dunefield changes may be relatively minor and independent of external sediment supply, owing to the counteractive geomorphic and sediment transport effects of the opposing winds. However, perfectly bimodal wind direction regimes represent a highly idealized end-member case, and SBDs in Grand Canyon with imperfect bimodal wind direction regimes (e.g., Fig. 2C) may undergo morphodynamic evolution based on whether a modern fluvial sediment supply exists and whether the wind regime ultimately transports more sediment towards, instead of away from, the dunefield.

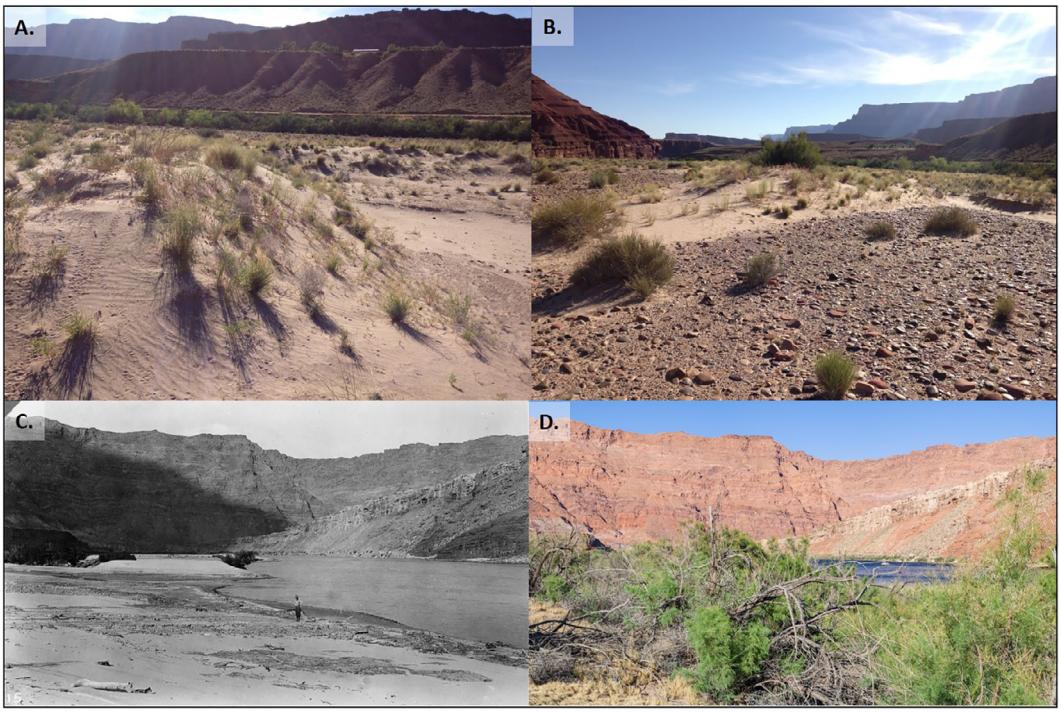

Fig. 4. Photos showing the A) interior and B) upwind extent of the Lees SBD in May 2017 (credit D. Solazzo). The dunefield is located on a cobble bar at the confluence of the Paria and Colorado Rivers and is considered to have a relict fluvial sediment supply. Matched photographs depict a large upwind source area of fluvial sand that was mostly bare in C) 1923 (Credit E.C. La Rue, U.S. Geological Survey Photographic Library, Denver, CO, USA), but densely vegetated with riparian shrubs in D) May 2017 (credit A. H. Fairley, U.S. Geological Survey).

obvious dune morphology in the SBDs suggests that those regions received abundant sand supply in the recent past, and thus SBDs may be places where sand accumulates most readily downwind from fluvial sand sources. Of the 117 total SBDs and ADAs, at least 53 are downwind of adjacent, contemporary subaerial sandbar deposits with varying degrees of riparian vegetation or topographic barriers that might partially impede aeolian transport (East et al., 2016) and therefore likely have a modern (i.e., post-dam), as opposed to relict (i.e., only pre-dam

or early post-dam), fluvial sediment supply.

The simplest conceptual model for SBDs that receive sediment from sandbars along the Colorado River in the Grand Canyon is that of transverse or barchanoid dunes that form in an approximately unidirectional wind regime that transports sediment from the upwind source area (e.g., a fluvial sandbar in an eddy or channel margin) towards the downwind dunefield. In this scenario, the predominant wind direction follows the path of the canyon and is either typically toward upstream, or alternatively toward downstream. Under more complex directional wind regimes, SBDs can be formed and resupplied with sand from multi-modal wind directions that alternately transport sand from subaerial deposits in eddies and channel margins.

We focused on three individual SBDs in the Grand Canyon with dune morphology that is visible in aerial imagery (Fig. 2). The Soap dunefield is at the confluence of Soap Creek with the Colorado River, 43 km downstream from Glen Canyon Dam, and is considered an SBD with modern fluvial sediment supply because of the presence of an adjacent, unvegetated fluvial sandbar immediately upwind of the aeolian dunes (Fig. 2A). The Lees dunefield is at the confluence of the Paria River with the Colorado River, 25 km downstream from Glen Canyon Dam, in an area known as Lees Ferry, and is considered an SBD with relict fluvial sediment supply because no modern sandbar or other fluvial sand source occurs upwind. However, photographs of the Lees dunefield from the early 1900s show that a fluvial sand deposit existed adjacent to, and upwind of, this SBD in the era before dam operations reduced the sediment supply to this reach of river and led to an increased density of riparian shrubs growing along the sandy shorelines (Figs. 2B and 4; also see Fig. 5 in Topping et al., 2003). The Fossil dunefield is at the confluence of Fossil Creek with the Colorado River, 227 km downstream from Glen Canyon Dam, and is considered an SBD with modern fluvial sediment supply because of the presence of an adjacent, but relatively small, downstream sandbar and upstream channel-margin fluvial sand deposits (Fig. 2C).

2.2. Numerical modelling

We used the Python implementation of Werner's (1995) dune model developed by Barchyn and Hugenholtz (2012) to illustrate the response of a synthetic SBD to endmember scenarios of unidirectional or bimodal upstream and/or downstream prevailing winds, and with or without upwind sediment source area(s) (Fig. 5).

2.2.1. Initial conditions DEM

In order to implement the wind and sediment supply scenarios, we first produced a synthetic digital elevation model (DEM) of an idealized dunefield based on modelled spatial patterns of erosion and deposition to use for initial conditions. This initial DEM (DEM_0) was evolved from an initially flat topographic surface by running the model for 11,110 iterations with a wind direction from the south (simulated wind direction toward upstream), with north and south periodic boundaries (in which cells leaving the northern boundary are added at the southern boundary), and no external sediment supply (the "slab thickness", or modelled sediment source, was set to 0 cells). The DEM (model domain) was 250 × 250 × 50 pixels in size, corresponding to the X, Y, and Z dimensions respectively.

2.2.2. Wind and sediment supply scenarios

We used the DEM_0 as input topography for modelling five different scenarios (Table 1): unimodal wind with (Scenario 1) or without (Scenario 5) upwind sediment supply, bimodal wind with (Scenario 3) or without (Scenario 4) downstream sediment supply, or bimodal wind with upstream and downstream sediment supply (Scenario 2). The five scenarios were modelled over two equal-interval model runs. For each model interval, we performed 1000 iterations, using a downstream and/or upstream wind direction from the south and/or north, respectively, without periodic boundaries, and with otherwise default parameters, with the exception of slab thickness. The number of new slabs imported on the upwind model boundary per iteration was set to 0 and 250 in the sediment-supply-absent and sediment-supply-present scenarios, respectively. In the sediment-supply-present scenarios 250 slabs were used because this value represented an average input of one slab per cell along the model boundary per iteration. A digital elevation model of difference (DOD) was produced by differencing each consecutive pair of model-run DEMs (DEM_0, DEM_1, DEM_2), which resulted in 2 DODs for each of the 5 scenarios. We completed the analyses with the 2 model runs and produced 2 DODs to illustrate the progression of changes at smaller intervals that led to the final net change. The DODs were summed for each scenario to produce a Sum of 2 DODs (SDOD) map showing the spatial distribution of net erosion and deposition in the simulated SBD. To summarize,

$$DOD_1 = DEM_1 - DEM_0 \quad (1)$$

$$DOD_2 = DEM_2 - DEM_1 \quad (2)$$

$$SDOD = DOD_1 + DOD_2 \quad (3)$$

The average topographic change per pixel (ΔZ) and the spatial patterns of erosion and deposition were summarized for each DOD to document the relative responses of the simulated dunefield to the wind and sediment supply scenarios.

2.3. Wind and sand drift potential analysis

We analyzed meteorological data collected at the Lees and Fossil sites over a six-year period to assess the magnitude and variability of winds with potential to transport sediment (site-specific meteorological data were not available for Soap; nor for most other SBDs in Grand Canyon). Wind speed and direction were measured 2.0 m above the bed, and summarized as 4-min averages of 3-s sampling intervals using a Vaisala WXT510/WXT520 weather transmitter with an ultra-sonic transducer (Caster et al., 2014). The complete weather data set, along with a detailed description of instrumentation, can be found in Caster et al. (2014) and associated data releases.

For this study, wind measurements were summarized for each station, when operational, between January 2010 and May 2016 (Caster et al., 2014). Wind speed summaries, including vector summation with mean and standard deviation wind directions (Yamartino, 1984) were plotted using only wind data where no rainfall was recorded within the previous 24 h (i.e. a very conservative estimate for presumed dry sand) at or above two transport threshold wind speeds (V_{t1} and V_{t2}; discussed below).

Sand-transport potential was estimated cumulatively over 1- and 5-year periods using Fryberger and Dean's (1979) drift potential. This method bins wind records into 16 equal-interval wind directions (Pearce and Walker, 2005) with nine velocity groups for each directional bin based on historical reporting criteria (Fryberger and Dean, 1979; Bullard, 1997). Following Fryberger and Dean (1979), we calculated drift potential (*DP*) using a modified equation from Lettau and Lettau (1978),

$$DP = \sum_{V_1}^{V_9} \sum_{t_{D1}}^{t_{D16}} V^2 (V - V_{t1}) * t_D, \ (V - V_{t1}) > 0$$

$$DP = 0, \ (V - V_{t1}) \leqslant 0 \quad (4)$$

where *DP* is the annual rate of potential sediment drift in vector units summed for each directional bin and velocity group. *V* is the velocity group mid-point, V_{t1} is the transport threshold wind speed of 6.17 m s^{-1} (12 knots; Fryberger and Dean, 1979), and t_D is the proportion of time wind is recorded in each velocity group and directional bin. This method is useful for providing *DP* values that can be directly compared to other dunefields globally evaluated by Fryberger and Dean (1979) and others since (e.g., Bullard, 1997). However, Pearce and Walker (2005) show that using the mid-point value for *V* within

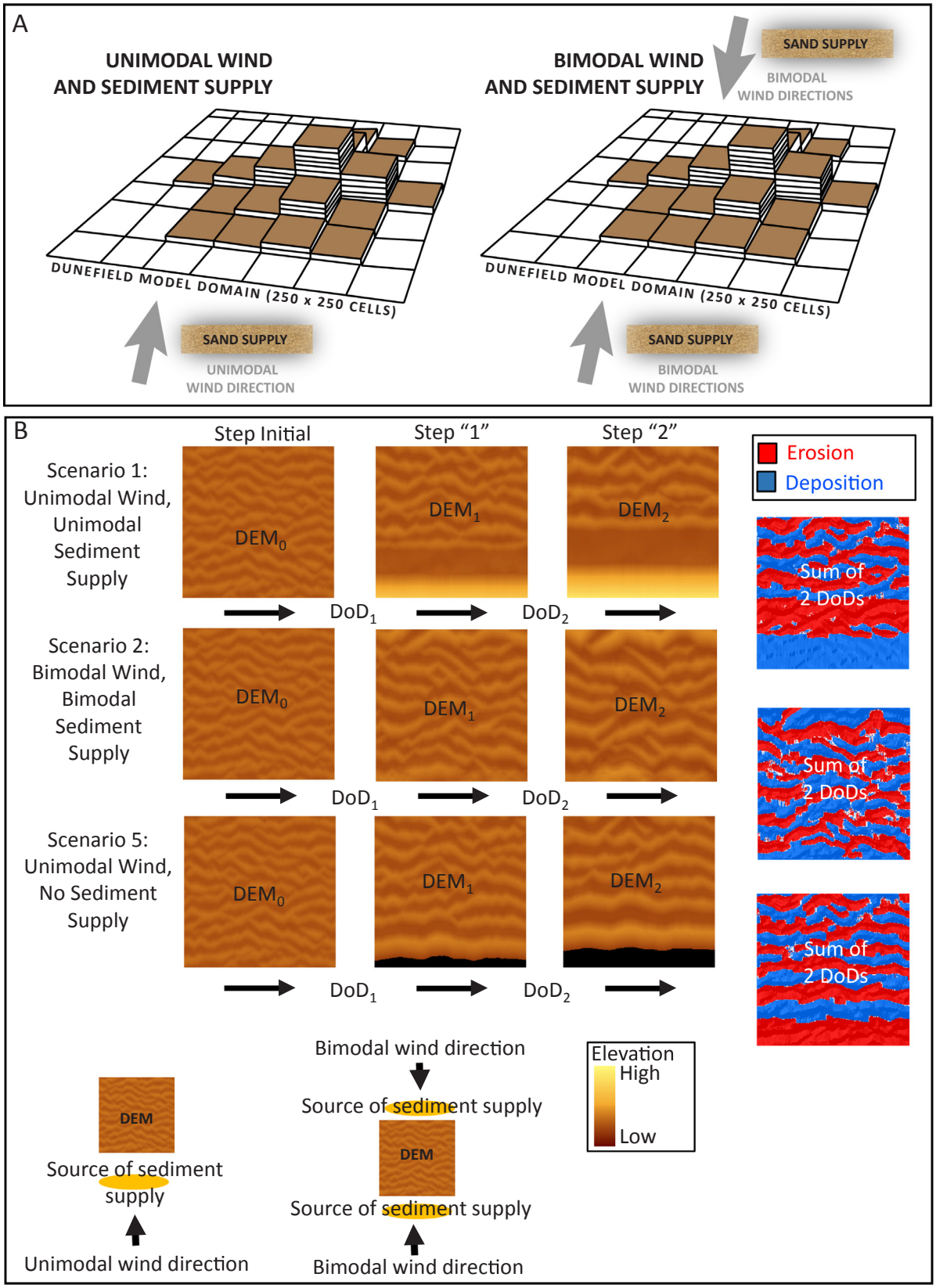

Fig. 5. Panel A) provides a conceptual illustration of the Barchyn and Hugenholtz (2012; modified with permission from Fig. 1) dune model (Werner, 1995) as applied to scenarios of upwind sediment source area(s) and either unidirectional or bidirectional prevailing winds. Panel B) depicts hypothetical dunefield response to these scenarios, as listed in Table 1. DEM refers to a Digital Elevation Model and DOD refers to DEM-of-Difference.

Table 1
Werner (1995) model scenarios and parameters (Barchyn and Hugenholtz, 2012).

Scenario	Sediment supply	Wind direction regime	Sediment source area
1	Yes	Unimodal	Upwind, downstream
2	Yes	Bimodal	Upwind, downstream and upstream
3	Yes	Bimodal	Upwind, downstream only
4	No	Unimodal	–
5	No	Bimodal	–

equation 1 typically results in overestimation of sediment transport. A more representative *DP*, hereafter termed DP_{local}, can be derived by replacing *V* using the mean or median of wind speed within the velocity and directional bins (Pearce and Walker, 2005). The use of a global average transport threshold (V_{t1}) has potential to overestimate or underestimate *DP* depending on local sediment grain characteristics (Bagnold, 1941). Therefore we additionally use a locally-derived transport threshold wind speed (V_{t2}) derived from Bagnold's (1941) formula for sand transport by,

$$V_{t2} = 5.75A\sqrt{\frac{\rho_s-\rho}{\rho}gd}\ln\left(\frac{z}{k}\right) \quad (5)$$

where *A* is a dimensionless constant equal to 0.1, ρ_s is the density of quartz sediment, ρ is the density of air, *g* is gravitational acceleration, *d* is the sediment grain diameter within dunefields in Grand Canyon (~0.221 mm; Draut and Rubin, 2008), *z* is the wind speed observation elevation, and *k* is the von Karman constant of 0.4.

Using these adjustments to Fryberger's model, DP_{local} is defined as,

$$DP_{local} = \sum_{Vm1}^{Vm9}\sum_{tD1}^{tD16} V_m^2(V_m-V_{t2})*t_{D,}\ (V_m-V_{t2}) > 0$$

$$DP_{local} = 0,\ (V_m-V_{t2}) \leqslant 0 \quad (6)$$

where V_m is the mean wind speed for each velocity and directional bin and V_{t2} is the local transport threshold wind speed (4 m s^{-1}; equivalent to the 2 m s^{-1} used by Draut and Rubin (2008), for measurements at a height of 2 m). We primarily focus our results and discussion on DP_{local} (as opposed to *DP*) for inter-site comparison relative to geomorphic change detection results.

As wind data was collected at 2 m above the bed rather than at Fryberger's standard instrument height of 10 m, wind-speed measurements were scaled using the modified Karman-Prandtl equation to transform the original data for calculation of *t* in Eqs. (4) and (6) and V_m in Eq. (6). The transformed velocity (V_{10}) was estimated as,

$$V_{10} = V_i\frac{\ln\left(\frac{Z_{10}}{Z_0}\right)}{\ln\left(\frac{Z_i}{Z_0}\right)} \quad (7)$$

where V_i is the measured (raw) wind speed at elevation z_i, z_{10} is the estimation elevation, and z_0 is a roughness length factor (Simiu and Scanlan, 1978). We applied a value of z_0 of 0.04 to all sites; this z_0 was found by Draut and Rubin (2008) to be representative of several sites where wind-velocity profiles were measured that were similar to the sites used in this study, i.e., sparsely vegetated dune localities with abundant open sand.

The resultant drift potential (*RDP*), defined as the vector sum of DP_{local}, is an estimate for the magnitude of sand drift along the resultant drift direction (*RDD*; opposite of wind vector angle). On a global scale, *DP* can be categorized into three groups based on Fryberger and Dean's (1979) criteria from wind speeds in knots and Bullard's (1997) metric equivalents (Table 2). On a site scale in Grand Canyon, DP_{local} provides a more representative ranking of spatio-temporal wind characteristics. The ratio of *RDP* to DP_{local} can be used to assess the complexity of winds and is comparable to the Yamartino (1984) standard deviation of wind direction. Where the *RDP* is equal to DP_{local}, directional variability in wind energy is low (strongly unimodal wind direction with low standard deviation of wind direction) and where *RDP* is substantially lower than DP_{local}, directional variability in wind energy is high (bimodal to multimodal wind direction with typically high standard deviation of wind direction; Table 2).

2.4. Decadal-scale geomorphic change detection

We compared results of the wind and sediment supply modelling scenarios to geomorphic change detection at the three SBDs in Grand Canyon. Change detection at all sites was conducted using 1 m resolution digital surface models (DSMs) acquired in 2002, 2009, and 2013. The DSMs, which differ from DEMs as vegetation was not removed from the remotely sensed elevation surface, were created by the data-acquisition contractor to the U.S. Geological Survey Grand Canyon Monitoring and Research Center from automated photogrammetry using 0.2 m resolution aerial imagery acquired via fixed wing aircraft and described in detail by Davis (2012, 2013) and Durning et al. (2016a,b). The DSMs have a previously reported inter-DSM vertical precision of 0.23 m among the three datasets, along with a nominal positional accuracy of 0.3 m (Kasprak et al., 2017). For this study, all three dates of DSMS were converted to point cloud datasets (using the raster cell centroids in ARCGIS) and the 2002 and 2013 DSMs point clouds were registered to the 2009 DSM point cloud using the CloudCompare fine registration tool (CloudCompare 2.8, 2017) focusing on sections of each DSM that were likely to have no significant topographic change during the inter-survey period (e.g., boulders and exposed bedrock). At each site, the DSM point cloud registration error, or root mean square error (RMSE) of elevation differences for all coincident points between 2002 and 2009 or between 2009 and 2013, was ≤0.11 m. The DSM point clouds were converted back to raster grids and then differenced, such that each consecutive pair of DSMs produced a DOD (i.e., $DOD_{2002\text{-}2009}$ and $DOD_{2009\text{-}2013}$). The two DODs for each site were also summed to produce an SDOD which was plotted to map net topographic change during the study period.

While the areal extents of change detection (henceforth termed "blocks") at Lees and Fossil were largely free of vegetation, small areas at the Soap site which included large woody shrubs were manually excluded from the change detection analysis. The DODs depict all elevation changes between the DSMs regardless of their vertical magnitude. We acknowledge that some areas of low-magnitude elevation change in the DODs may be the product of either sparsely distributed low stature vegetation or survey noise, and not geomorphic processes driving elevation changes (Wheaton et al., 2010). At the same time, we chose not to threshold out low-magnitude elevation changes because here we are primarily concerned with interpreting dune morphology and migration, and thus we wanted to preserve the spatial patterns of erosion and deposition in DODs whenever possible. For practical purposes, an estimate of our minimum level of change detection (that is, the smallest magnitude of elevation change that we can reliably distinguish from survey noise) in the DODs can be computed by propagating DSM registration error (0.11 m) as the sum of squares in quadrature (Lane et al., 2003; Kasprak et al., 2017), which yields a minimum level of detection of 0.15 m. Note that while this estimate represents the smallest vertical change we can reliably distinguish on a pixel-by-pixel basis, volumetric sediment budgets may be below this threshold for sites at or near sediment equilibrium and still be significant with respect to minimum detection limits, as net volumetric change is simply computed by summing all change pixels across a DOD (or sub-block therein). Sankey et al. (2018) demonstrate an alternative approach, wherein uncertainty in topographic change can be incorporated into the change detection results on a spatially-continuous basis.

To visualize patterns of dune migration associated with wind

Table 2
Wind regime classifications based on drift potential after Fryberger and Dean (1979; Bullard, 1997).

Fryberger's Wind Environment Categories		Fryberger's Global *DP* Categories (knots)	Bullard's Global *DP* Categories ($m\,s^{-1}$)	Fryberger's *RDP/DP*
Energy	Low	< 200	< 27	–
	Intermediate	200–400	27–54	–
	High	> 400	> 54	–
Directional Complexity	Complex to obtuse bimodal	–	–	< 0.3
	Obtuse bimodal to acute bimodal	–	–	0.3– < 0.8
	Wide unimodal to narrow unimodal	–	–	> 0.8

transport, we constructed profiles for each DOD along the expected wind transport direction. This direction corresponds to the *RDD* in the case of Lees and Fossil, and to a longitudinal trace through the dunefield perpendicular to the average dune crest orientation at Soap (which we infer to be the dominant wind direction, in the absence of direct wind measurements, based on our experience working in the field and conducting remote sensing at this site).

Topographic (vertical) changes along the *RDD* were averaged within 50-m long sub-blocks using the entire width of the sub-block within each DoD; 50 m is approximately equivalent to the minimum length scale of at least one complete dune crest and trough, (i.e., the crest-to-crest distance or dune period) at each site. These vertical changes were then expressed as mean volumetric change (ΔV) per 50 m long sub-block with unit (1 m) width. ΔV was divided by 11 years to express the changes as a mean annual volumetric sediment flux during the change detection period. A positive value for the mean annual volumetric sediment flux implies that the flux of sediment into the sub-block was greater than flux out of the sub-block (i.e., aggradation), whereas a negative mean volumetric sediment flux implies net sediment loss, or degradation.

3. Results

3.1. Werner dune model wind direction and sediment supply scenarios

Under scenario 1 with unimodal (upstream) wind and strong sediment supply, a transverse or barchanoid dune forms at the upwind edge of the simulated dunefield, causing that portion of the dunefield to aggrade (Fig. 5B). Between the modelling steps, dunes migrated downwind away from the sediment source area and also coalesced into fewer, larger dune crests and troughs (Fig. 5B). The spatial patterning of dune crests and troughs appears as areas of net deposition or erosion that were elongated perpendicular to the prevailing wind in the DEMs and SDODs (Fig. 5B). As a whole, the dunefield aggraded more under scenario 1 than any of the other modelled wind and sediment-supply scenarios (Fig. 6)

Conversely, under scenario 5 with unimodal wind but no sediment supply, an area of erosion forms at the upwind edge of the dunefield causing that portion of the dunefield to deflate (Fig. 5B). However, similar to the downwind portions of the dunefield in scenario 1, dunes migrated downwind away from the sediment source area and also coalesced into fewer, larger dune crests and troughs (Fig. 5B). Dune crests and troughs and areas of net erosion or deposition were elongated perpendicular to the prevailing wind (Fig. 5B). The dunefield as a whole deflated more under scenario 5 than in any of the other modelled wind and sediment supply scenarios (Fig. 6).

Under scenarios 2–4, with bimodal wind regimes and with or without sediment supply, more subtle areas of erosion or deposition at the upwind edges of the dunefields occur without and with sediment supply, respectively (Fig. 5B; note only scenario 2 shown). Away from the edges of the DEMs and the SDODs, the spatial patterning of dune crests and troughs, and areas of net erosion or deposition, are elongated perpendicular to the bimodal winds (Fig. 5B). As a whole, the dunefield aggraded under the bimodal and unimodal sediment-supply scenarios 2 and 3, and deflated under the no-sediment-supply scenario 4 (Fig. 6).

3.2. Wind and sand drift potentials

Fryberger's drift potentials (Fryberger and Dean, 1979) based on wind measurements made in $m\,s^{-1}$ were 4.7 at Fossil and 7.0 at Lees. Both sites are therefore low wind energy relative to other dunefields around the world (Table 2). We present wind roses and DP_{local}, *RDP*, *RDD*, and RDP/DP_{local} estimates for each site in Fig. 7. Based on DP_{local}, Lees is approximately a 30% higher energy environment as compared to Fossil. The directional complexity of the wind regime is greater and clearly more multi-modal at Fossil, and is much more unimodal at Lees. At Fossil, the wind blows upstream, downstream, and inland from the river channel towards the debris fan and SBD, with an *RDD* in the inland direction. At Lees, wind blows predominantly toward the upstream direction. We assume that wind also blows predominantly toward upstream at Soap, based on the morphology of the barchanoid dunes at the site (Fig. 2A).

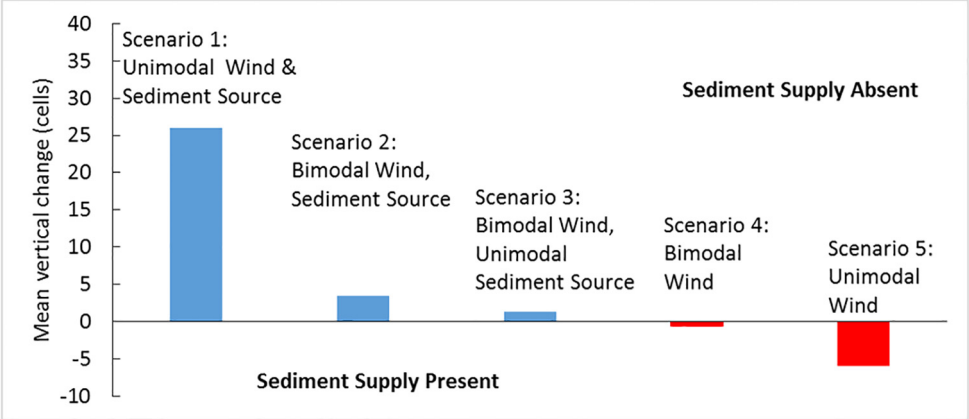

Fig. 6. Modelled sediment imbalance for the sum of DODs (SDOD) produced with the five different Werner model (1995; Barchyn and Hugenholtz, 2012) scenarios.

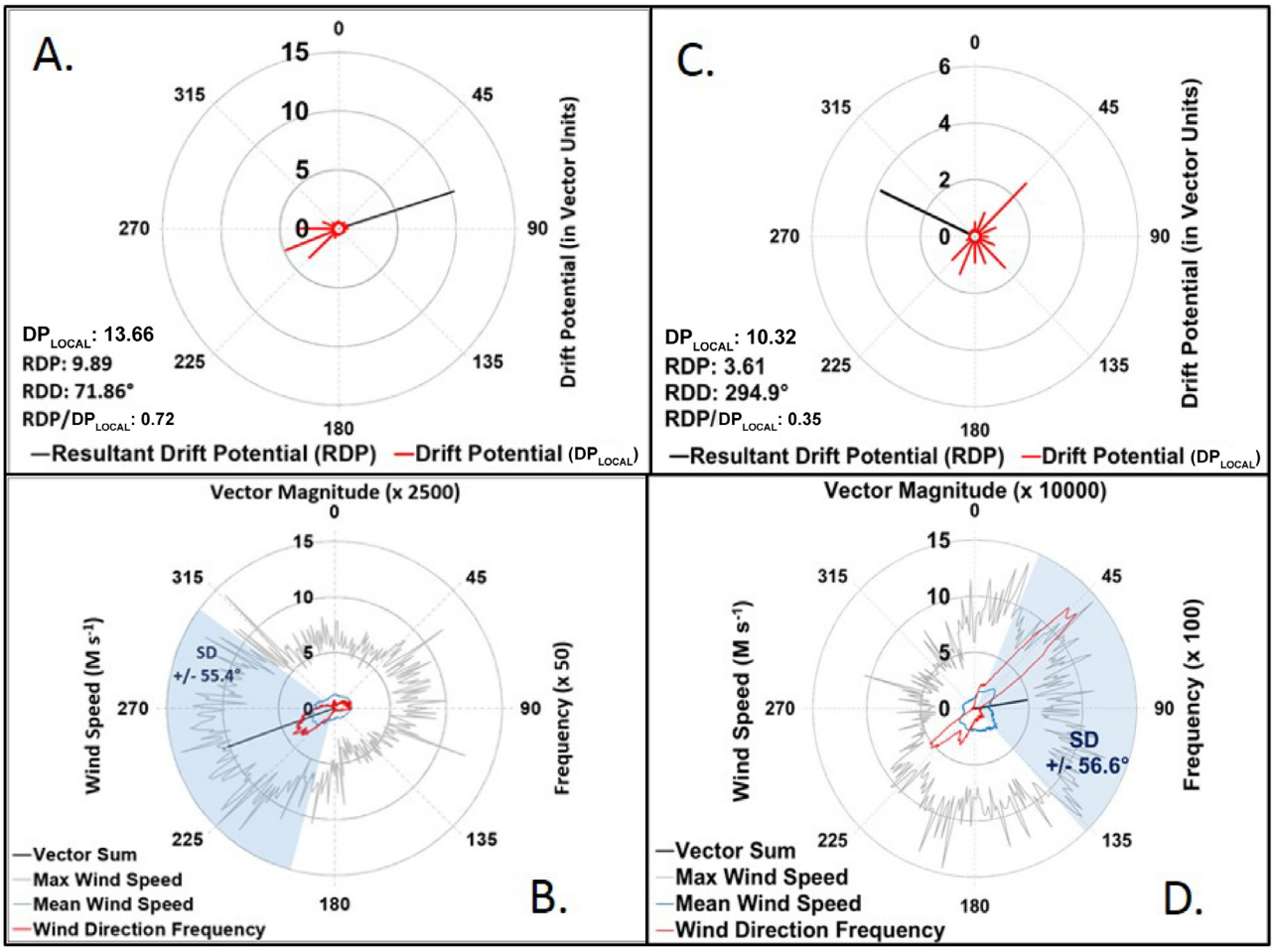

Fig. 7. Wind and sand rose diagrams for two of the three differing source-bordering aeolian dunefields along the Colorado River in Grand Canyon. A) and B) are the sand and wind roses, respectively, from a weather station located in the Lees SBD. C) and D) are from the Fossil SBD. Note that the Soap SBD is located 18 km downstream from Lees and based on dune morphology and the authors' field experience is considered to have a relatively unimodal wind regime comparable to Lees though with different *RDD*.

3.3. Hypothesis testing using geomorphic change detection data

During the two change detection intervals, the Soap dunefield with unimodal wind regime and modern fluvial sediment supply aggraded in the upwind half of the dunefield, and deflated in the downwind half of the dunefield (Figs. 8A, 9A). The mean volumetric sediment flux for the four 50-m sub-blocks ranged from 0.1 to $-0.2\,m^3/y$ (Fig. 9A), and indicated that the flux into the two most upwind sub-blocks exceeded the flux out, whereas the opposite was true for the two most downwind sub-blocks. Individual dune crests and troughs in the two DODs migrated distances of 8–12 m along the longitudinal profile plotted in Fig. 9A. The measured aggradation and deflation at individual dune crests and troughs ranged from 0.9 m to −1.2 m (along the longitudinal profile in Fig. 9A). These observations support H1.

The Lees dunefield, with unimodal wind regime and no modern fluvial sediment supply, deflated throughout each of the five 50-m sub-blocks surveyed, and the mean volumetric sediment flux for the sub-blocks ranged from -0.03 to $-0.4\,m^3/y$, indicating that the flux out of each sub-block exceeded the flux in (Fig. 8B, 9B). Individual dune crests and troughs in the two DODs migrated distances of 8–16 m along the longitudinal profile plotted in Fig. 9B. The measured aggradation and deflation at individual dune crests and troughs ranged from 0.8 to -1.4 m (along the longitudinal profile in Fig. 9B). These observations support H2.

The Fossil dunefield, with multi-modal wind regime, deflated in each of the 50 m sub-blocks for both upstream and downstream portions of the dunefield, and the mean volumetric sediment fluxes ranged from -0.1 to $-0.6\,m^3/y$ (Fig. 8C and 9C, D; Block A is upstream and Block B is downstream). The SDODs at Fossil (Fig. 8C) show dunes in the middle of both blocks of the dunefield with areas of erosion and deposition oriented approximately orthogonal to the *RDD*. However, migration of multiple individual dune crests and troughs between the two DODs is not visible along the longitudinal profile of the *RDD* (Fig. 9 C, D). Along the longitudinal profile of the *RDD*, the middle of Block A aggraded primarily between 2002 and 2009, but then deflated more between 2009 and 2013 (Fig. 9C). The upwind and middle parts of Block B deflated between 2002 and 2009 and then aggraded between 2009 and 2013, along the longitudinal profile of the *RDD* (Fig. 9D). These observations reject a portion of H3, specifically that the dunefield would aggrade along the upwind end of the *RDD* path. Thus we infer that the dunefield did not have sufficient external sediment supply to drive aggradation at the upwind edge of the SBD. However, the observations support the second portion of H3, that the dunefield would not show clear evidence of directional migration of individual dunes along the *RDD*.

4. Discussion and conclusion

SBDs are widely occurring geomorphic landforms in arid and semi-arid regions globally, and are sensitive to changes in climate and land use (Fryberger and Dean, 1979; Davidson-Arnott and Law, 1990; Bullard and McTainsh, 2003; Wiggs et al., 2003; Rendell et al., 2003;

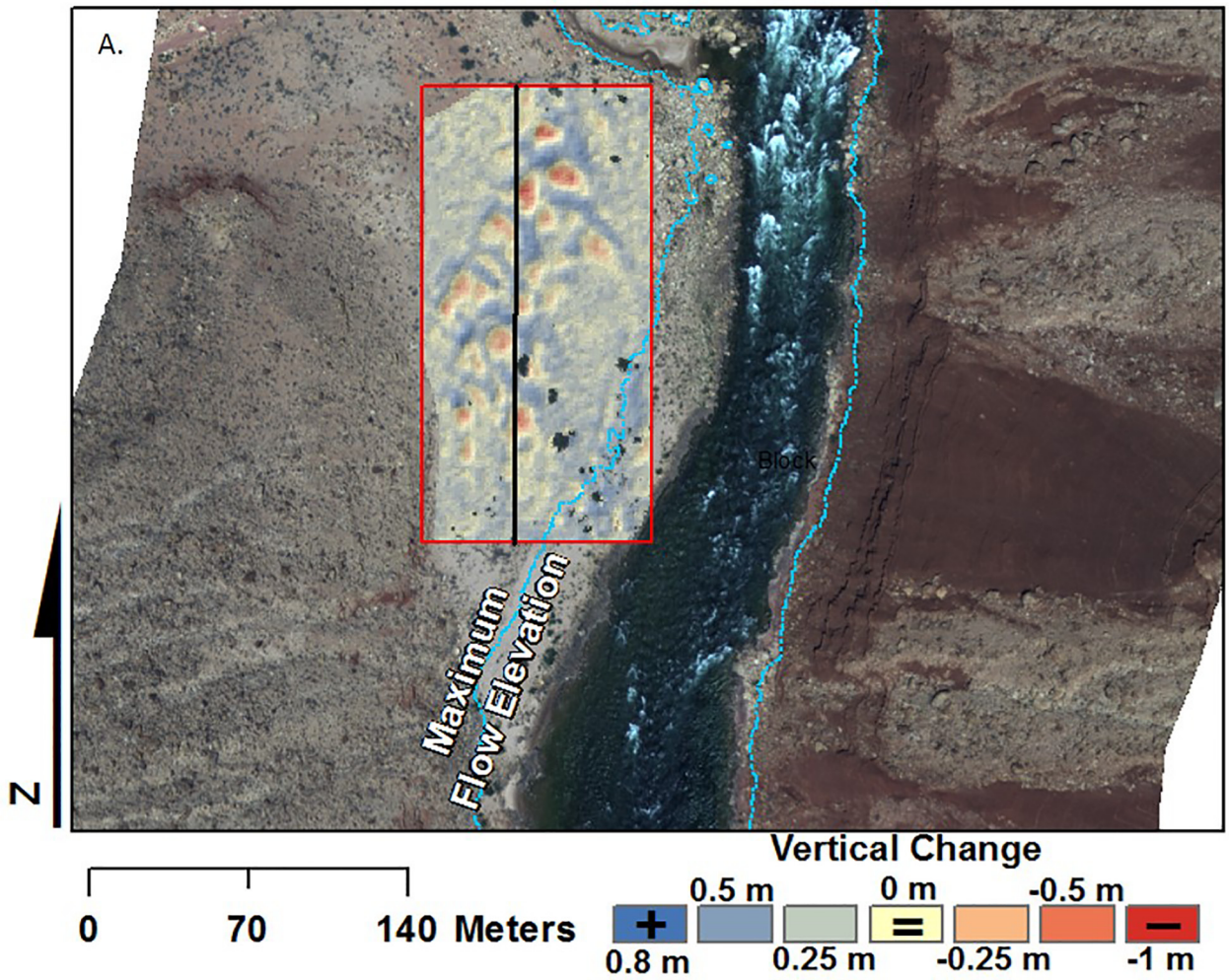

Fig. 8. Sum of two Digital Elevation Models of Difference (SDOD) spanning 2002–2013 for the three source-bordering aeolian dunefields along the Colorado River in Grand Canyon with differing wind directions and sediment supply. A) Soap; B) Lees; C) Fossil. Maximum flow elevation denotes area inundated by river flows during 2002–2013. The rectangle outlined in red shows the entire extent of the block within which volumetric changes were examined at each dunefield and summarized in Fig. 9. The black line is drawn parallel to predominant wind (e.g., *RDD*) and shows the path traced by the longitudinal profiles of topographic changes presented in Fig. 9. Each SDOD is presented as a hillshade GIS layer classified with red and blue colors that indicate inferred aeolian erosion and deposition, respectively, during the 11 year change detection time period. In the SDODs, downwind alternating patterns of red and blue highlight aeolian geomorphic changes including dune migration as well as features such as blowouts, dune troughs, and dune crests.

Hesp et al., 2005, May, 2014; Bogle et al., 2015; Liu and Couthard, 2015; Al-Masrahy and Mountney, 2015). In river valleys, aeolian landscapes such as SBDs are sensitive to changes in river hydrology, and they develop and evolve as a function of the supply of fluvially sourced aeolian sediment (Page, 1971; Page et al., 2001; Al-Masrahy and Mountney, 2015; Han et al., 2007; Draut, 2012; Rendell et al., 2003). SBDs currently exist along the Colorado River in the Grand Canyon in locations where river sediment resupply varies due to local landscape characteristics and the contemporary regulated hydrologic and sediment regime (Draut, 2012). Despite the observed response of SBDs to alterations in sediment supply owing to river regulation by dam operations, an analytical framework for using observational data to infer spatiotemporal sediment resupply along the Colorado or other similar rivers around the world has not been developed prior to this study.

We used numerical modelling, analysis of wind, analysis of sand drift potential, and remote-sensing change detection to evaluate a theoretically based framework in which sediment resupply to SBDs is inferred from patterns of topographic change and the local wind regime. As hypothesized, the SBD at our Soap Creek study site aggraded and thus received new sediment during the decadal change detection period, whereas the relict SBD Lees at the Paria River deflated, and thus was not resupplied with sediment. The Soap and Lees dunefields have unimodal wind regimes with well-defined barchanoid dune morphology. Fossil, previously considered a modern-sourced SBD (East et al., 2016), though with small potential upwind sediment source areas (Fig. 2C), showed geomorphic changes suggesting it was not significantly resupplied with sediment during the 11-year study period.

The results of numerical modelling (Section 3.1) and analysis of wind and sand drift potential (Section 3.2) suggest that the approach to inferring morphodynamic response via geomorphic change detection (Section 3.3) to sediment-supply changes in SBDs should differ depending on wind regime. At sites with strongly unimodal wind regimes, prior studies of aeolian bedform evolution indicate that the orientation of dune crests and troughs is less sensitive to directional variability in sand transport because the divergence angle between transport directions is small (e.g., < 90 degrees; Rubin and Hunter, 1987; Rubin, 2012). Thus it is generally reasonable to expect transverse dunes to persist and migrate downwind of the fluvial sandbars or channel margins in environments like Soap or Lees. Conversely, in environments with a multimodal wind regime such as Fossil, transverse dunes are not necessarily expected to persist and migrate downwind relative to either the upstream, downstream, or inland (*RDD*) winds. The orientation of

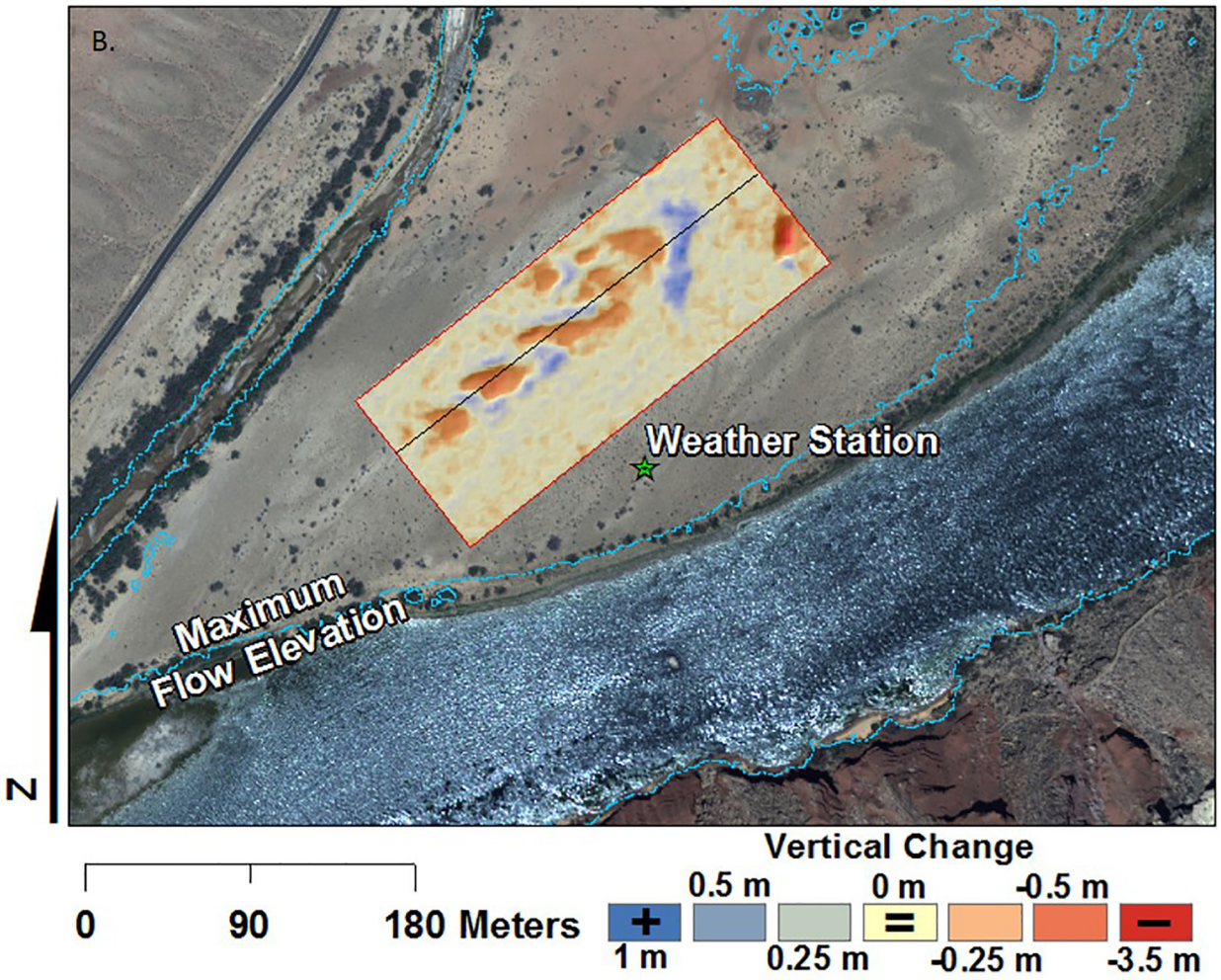

Fig. 8. (*continued*)

dune crests and troughs is sensitive to directional differences in sand transport because the divergence angle between directions of transport is large in such environments (e.g., near 180 degrees; Rubin and Hunter, 1987; Rubin, 2012). The bimodal numerical modelling scenarios were idealized cases in which the divergence angle between directions of transport is exactly 180 degrees, and transverse dunes are thus overprinted and/or eroded with each change in the modelled wind direction (Fig. 5). The idealized bimodal scenarios are useful, however, in demonstrating that under widely varying wind direction regimes, SBDs (or some portion thereof) should aggrade when a significant external sediment supply exists (Fig. 6) even if the spatial and directional patterns and migration of individual dunes cannot be deciphered from morphodynamic analysis.

It is important to acknowledge several real-world caveats to invoking either the numerical modelling or the wind regime analysis to explain dune forms and morphodynamics in complex terrain with sparse vegetation. For example, under unidirectional flow conditions, the numerical approach models transverse dune evolution via mechanisms of fallout deposition and lee slope avalanching (Werner, 1995; Barchyn and Hugenholtz, 2012), but does not account for flow deflection in the lee of transverse dunes than can transport sediment parallel to the bedform (Walker et al., 2006; Walker and Shugar, 2013). The Fryberger method for drift potential analysis (Fryberger and Dean, 1979) provides a geographically coarse assessment of net aeolian sediment drift vector and variability, but was developed to relate to regional dune morphology in unvegetated desert settings with limited confounding (non-dunefield) topography. Thus, it also does not accommodate secondary flow and transport patterns – over transverse dunes for example – nor areas where vegetation influences dune development (Walker et al., 2006; Walker and Shugar, 2013). Our change detection results do show clear examples of barchanoid dune forms at Lees and Soap as well as migration of some of these dunes relative to the measured or inferred *RDD* (Figs. 8 and 9). At Fossil, where sand drift potential analysis indicates that flow is more directionally complex, there are some dunes in the SDOD that appear to have migrated roughly in the direction of the *RDD* (Fig. 8), but the volumetric sediment fluxes in Fig. 9 don't indicate an along-*RDD* import of net sediment into the dunefield, nor do the longitudinal profiles in Fig. 9 show any clear examples of dune migration. At all sites, we acknowledge that wind flow and sediment transport could be directionally complex – for example within individual lee slopes, interdune areas, or blowouts, or near riparian shrub vegetation along the river channel (Walker et al., 2006; Walker and Shugar, 2013; Abhar et al., 2015) – in ways that affect variability in morphodynamic-based sediment budgets that we are currently not able to explain.

The relict SBD Lees is on a gravel bar at the confluence of the Paria and Colorado Rivers (Fig. 4), which, prior to regulation of the Colorado River, was dissected by channels of both rivers and more frequently inundated by river flows (Topping et al., 2003). During pre-dam times, an SBD likely formed at this location during periods of low river flow from aeolian transport of flood sand originally deposited by the Colorado or Paria River within the otherwise coarse-grained bar sediments. During floods of the Paria or Colorado Rivers that inundated the bar, the SBD was probably either eroded by the river flows or buried by

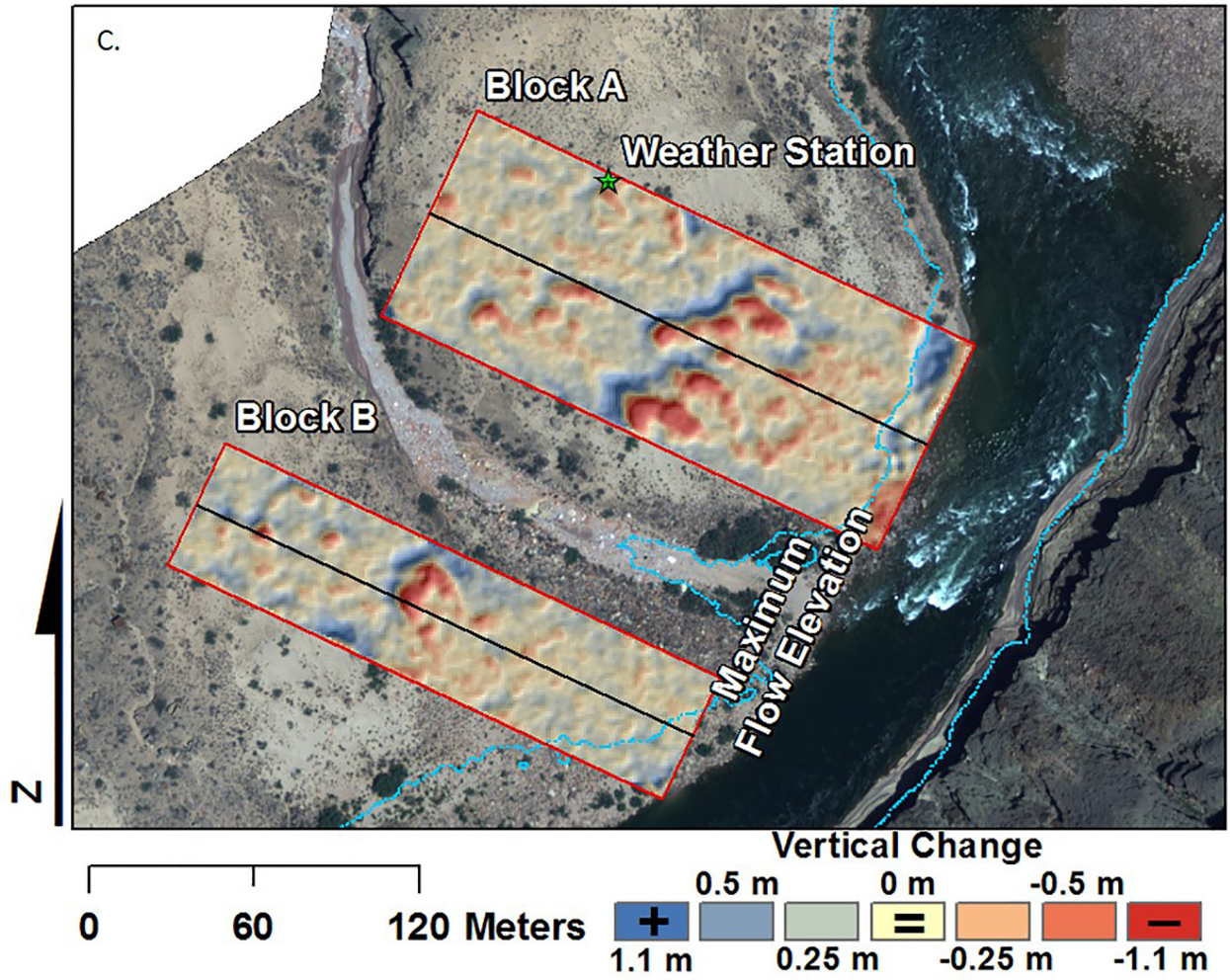

Fig. 8. (*continued*)

flood sediments. The current SBD at Lees is sediment-starved because the Colorado River no longer inundates the bar and therefore does not resupply the sand deposits due to regulation of river flow by the dam since 1963; additional sediment-supply limitation may have been imposed by a levee constructed in the early 1980s (Topping et al., 2003). This SBD is also currently sediment-starved because the channel of the Paria River and the sandy shoreline at the confluence of the Paria and Colorado Rivers has become densely vegetated with woody riparian shrubs during the past five decades (Fig. 4C, D; Sankey et al., 2015).

The SBD at Soap, which does receive modern sediment supply, is located along the toe of a debris fan formed as the Soap Creek tributary enters the Colorado River. A majority of the area of the current Soap SBD was inundated by the largest floods (up to 5940 m^3/s; Magirl et al., 2008) of the Colorado River prior to regulation (Fig. 10A, B). The largest post-dam floods during the early 1980 s (up to 2747 m^3/s) also inundated roughly half of the area of the current SBD, however the largest floods since then (up to 1274 m^3/s) only have inundated the extent of the sandbar that is the current upwind source area for the Soap SBD (Magirl et al., 2008). Therefore, during large floods prior to river regulation and during the largest floods post-regulation, the area was probably intermittently eroded by river flows or buried by flood deposits, although like Lees, an SBD formed during periods of low river flows with abundant upwind sand supply. More recently, dam-controlled floods in 1996, 2004, 2008, 2012, 2013, 2014, and 2016, although smaller than the annual pre-dam spring flood, have generally resupplied the upwind sandbar with sediment, which in turn has permitted sediment resupply to the Soap SBD, such as during the 2002–2013 time period that we analyzed.

The SBD at Fossil has previously been considered to have some modern sediment supply because of the nearby sandy river shorelines in a downstream eddy and upstream channel margin locations (East et al., 2016; Collins et al., 2016), although like Lees, riparian shrubs cover the shorelines much more densely now than during the pre-dam era (Fig. 10C, D). Fossil has a complex wind regime that theoretically could resupply the dunefield with sand from any or all of those source areas. Some portions of the dunefield, at least along the margins, should have aggraded if the dunefield were resupplied throughout the decade of our analysis. However, the dunefield deflated on average, indicating a lack of supply sufficient to drive aggradation at the upwind edges of the SBD over the 11 years. Therefore, Fossil either does not have a modern sediment supply as previously surmised, or perhaps aggradation may occur as a threshold response (Schumm, 1979) to upwind sediment supply, and thus may occur only when supply exceeds a certain magnitude in the adjacent sandbar (i.e., a threshold not exceeded from 2002 to 2013 at Fossil), for example. Most of this large dunefield is at higher elevation relative to the river compared to the Lees and Soap SBDs, and was not inundated by even the largest pre-dam river floods of record (up to 5940 m^3/s; Magirl et al., 2008). In spite of the elevation difference relative to the contemporary river channel and the small size of the various upwind sand source areas, the Fossil SBD probably continues to persist because the opposing upstream, downstream, and inland wind directions keep more sediment within the dunefield, in contrast to a sediment-starved SBD with strong unidirectional wind regime, for example, in which dunes can ultimately migrate downwind

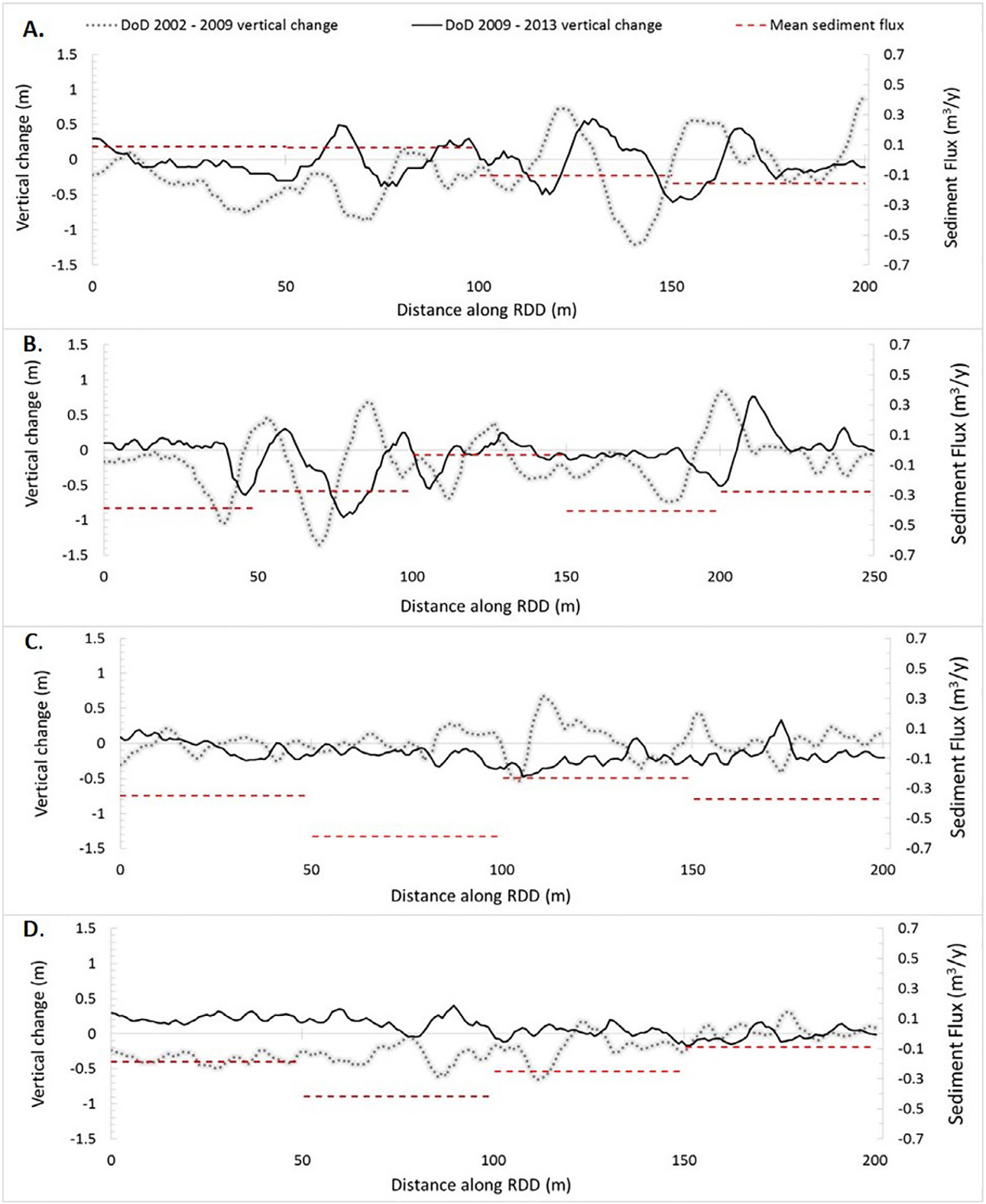

Fig. 9. Panels show topographic change detection results from: A) Soap. B) Lees. C) Block A at Fossil (see Fig. 8C). D) Block B at Fossil (see Fig. 8C). In each panel, the gray dashed line and black solid line show topographic (vertical) changes along longitudinal profiles perpendicular to dune crests (i.e., parallel to predominant wind; *RDD*; illustrated in Fig. 8) from DODs at the three differing source-bordering aeolian dunefields along the Colorado River in Grand Canyon. In each panel, the red dashed line shows mean sediment flux determined from volumetric change results in the SDOD summarized by 50-m long sub-blocks that extended the width of the block outlined by the red rectangle at the corresponding site in Fig. 8.

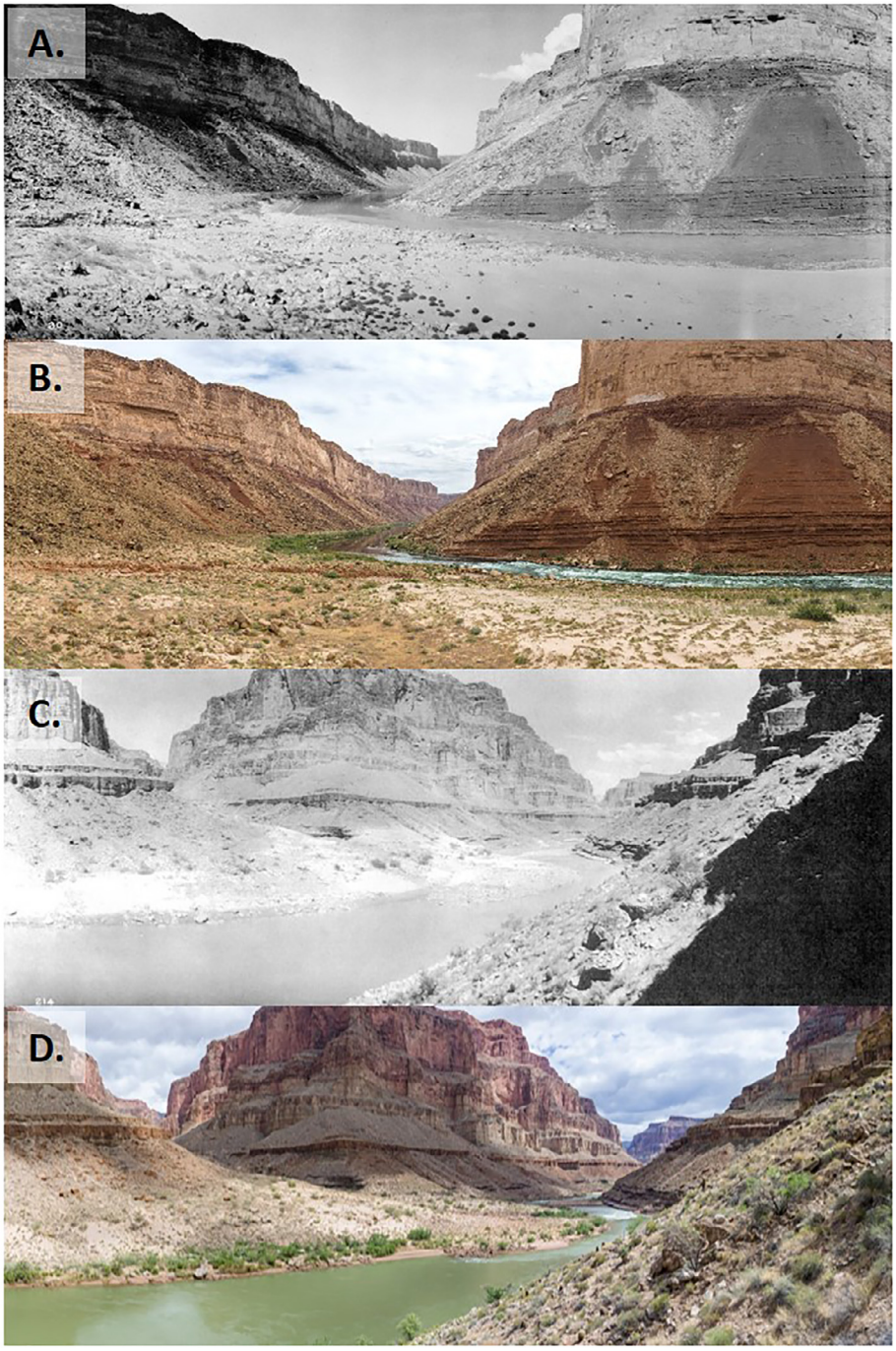

Fig. 10. Photos showing approximately half (downwind portion) of the SBD at Soap in A) 1923 and B) May 2017 (Photo Credits: A. H. Fairley, May 2017, U.S. Geological Survey; E.C. La Rue, 1923, U.S. Geological Survey Photographic Library, Denver, CO). Most of the area covered by the Soap dunefield was probably inundated by the largest floods (up to 5940 m^3/s; Magirl et al., 2008) of the Colorado River prior to regulation (pre-1963), whereas the largest post-regulation floods during the early 1980 s (up to 2747 m^3/s) inundated roughly half of the area of the current SBD, and the largest floods since then (up to 1274 m^3/s) have not inundated it. C) and D) show the Fossil SBD in 1923 and May 2017, respectively (Photo Credits: A. H. Fairley, U.S. Geological Survey, May 2017; E.C. La Rue, 1923, U.S. Geological Survey Photographic Library, Denver, CO). Note the increase in riparian vegetation along the sandy river shorelines between C and D.

and out of the SBD (and into the river or a tributary channel).

This work builds upon the rich history of geomorphic and sediment-transport studies in Grand Canyon, particularly with regard to spatially extensive, high resolution topographic datasets such as the DSMs used here. We intend for this analytical framework to be extendible to other river valleys that house SBDs around the world, given that such high-resolution topographic data are becoming ubiquitous in the Earth sciences (Kasprak et al., 2012; Westoby et al., 2012; Fonstad et al., 2013; Wheaton et al., 2013, 2015; Williams et al., 2014; Bangen et al., 2016). The extraction of information on fluvial and aeolian morphodynamics from topographic datasets in lieu of, or in concert with, direct field measurement of sediment transport rates, is increasingly commonplace, and removes some of the logistical barriers and high uncertainty inherent in measuring sand transport directly in the field as a means to infer morphodynamic evolution (Bauer et al., 1996; Grams et al., 2013; Kasprak et al., 2017; Leyland et al., 2017). Moreover, at higher data resolutions it may be possible to solve directly for the boundary sediment flux entering and exiting a given SBD, thereby eliminating the need for using overall net volume change as a surrogate for sediment supply and allowing for a direct classification of SBDs based on a quantification of sediment supply (for more information see Vericat et al., 2017). We foresee our approach as being beneficial to researchers and river managers working in dryland settings, particularly as new remote-sensing and meteorological data acquisition allows this conceptual approach to be applied to a wider range of SBDs with varying degrees of wind regimes, sediment resupply frequency and magnitude, and degrees of river flow and sediment alteration.

In this study, we have demonstrated an approach to infer the response of individual aeolian source-bordering dunes to variability in sediment supply during discrete time periods along the Colorado River

in Grand Canyon. The Colorado River is one of the most intensively managed rivers in the world, where a primary focus of river management is the use of periodic, sediment-rich controlled floods to maintain and redistribute sand throughout an otherwise sediment-starved river system. River managers wish to know how SBDs in turn vary as a function of specific management activities like controlled floods. The approach we present can be applied to shorter time periods with high resolution topographic data that bracketed individual controlled floods, for example, to infer the response of SBDs to such events (see Sankey et al., 2018). Such an applied methodology could also be useful for measuring sediment connectivity and associated anthropogenic alterations in connectivity in other dryland river settings around the world. Finally, we suggest that a refined understanding of the role of sediment supply in controlling landscape evolution in SBDs is vital for assessing changes to ecosystems that occur indirectly from anthropogenically induced loss of sediment supply. Because SBDs that lose sediment supply can become colonized by vegetation and biological soil crust as dune mobility decreases (Draut, 2012), in turn promoting important changes in carbon and nitrogen cycling as well as vascular plant growth (Harper and Belnap, 2001; Elbert et al., 2012; Viles, 2012), quantifying changes in dune mobility and activity within SBDs is essential to measuring changes in habitat characteristics within aeolian landscapes, likely a promising direction for future dryland research.

Acknowledgements

This research was funded by the Bureau of Reclamation's Glen Canyon Dam Adaptive Management Program, with additional funding from a National Science Foundation award to the National Center for Earth Surface Dynamics at the University of Minnesota, Minneapolis, MN. Support was also provided by the USGS Mendenhall Fellowship program to A. Kasprak. The authors acknowledge the Grand Canyon National Park for providing permission to conduct field research. The authors thank Jan Balsom, Mary Barger, David Bedford, Brian Collins, Skye Corbett, Jen Dierker, Paul Grams, and Jack Schmidt for help and discussions in the field and the office that greatly improved the research and the manuscript. Brian Collins, Skye Corbett, Terry Arundel, and Tom Gushue helped to archive the geospatial data for this project. Boatmen Carolyn Alvord, Don Baco, Kirk Burnett, Seth Felder, Dennis Harris, Don Massman, and Mark Perkins were instrumental in safely navigating the Colorado River during the many trips that generated the data used in this study. This manuscript is submitted for publication with the understanding that the US Government is authorized to reproduce and distribute reprints for Governmental purposes. Any use of trade, product, or firm names is for descriptive purposes only and does not imply endorsement by the US Government.

References

Abhar, K.C., Walker, I.J., Hesp, P.A., Gares, P.A., 2015. Spatial-temporal evolution of aeolian blowout dunes at Cape Cod. Geomorphology 236, 148–162.
Al-Masrahy, M.A., Mountney, N.P., 2015. A classification scheme for fluvial–aeolian system interaction in desert-margin settings. Aeolian Res. 17, 67–88.
Bagnold, R.A., 1941. The Physics of Blown Sand and Desert Dunes. Methuen, London, pp. 265.
Bangen, S., Hensleigh, J., McHugh, P., Wheaton, J., 2016. Error modeling of DEMs from topographic surveys of rivers using fuzzy inference systems. Water Resour. Res. 52 (2), 1176–1193.
Barchyn, T.E., Hugenholtz, C.H., 2012. A new tool for modeling dune field evolution based on an accessible, GUI version of the Werner dune model. Geomorphology 138, 415–419.
Bauer, B.O., Davidson-Arnott, R.G.D., Nordstrom, K.F., Ollerhead, J., Jackson, N.L., 1996. Indeterminacy in aeolian sediment transport across beaches. J. Coastal Res. 12, 641–653.
Bauer, B.O., Davidson-Arnott, R.G.D., Hesp, P.A., Namikas, S.L., Ollerhead, J., Walker, I.J., 2009. Aeolian sediment transport on a beach: surface moisture, wind fetch, and mean transport. Geomorphology 105, 106–116. http://dx.doi.org/10.1016/j.geomorph.2008.02.016.
Belnap, J., 2012. Unexpected uptake. Nat. Geosci. 5, 443–444.
Bogle, R., Redsteer, M.H., Vogel, J., 2015. Field measurement and analysis of climatic factors affecting dune mobility near Grand Falls on the Navajo Nation, southwestern United States. Geomorphology 228, 41–51.
Bullard, J.E., 1997. A note on the use of the "Fryberger method" for evaluating potential sand transport by wind. J. Sediment. Res. 67, 499–501.
Bullard, J.E., McTainsh, G.H., 2003. Aeolian-fluvial interactions in dryland environments: examples, concepts, and Australia case study. Prog. Phys. Geog. 27, 471–501.
Caster, J., Dealy, T., Andrews, T, Fairley, H., Draut, A., Sankey, J.B., 2014. Meteorological data for selected sites along the Colorado River Corridor, Arizona, 2011–13: U.S. Geological Survey Open-File Report 2014-1247, 56 p.
Collins, B.D., Bedford, D.R., Corbett, S.C., Cronkite-Ratcliff, C., Fairley, H.C., 2016. Relations between rainfall–runoff-induced erosion and aeolian deposition at archaeological sites in a semi-arid dam-controlled river corridor. Earth Surf. Process. Land. 41 (7), 899–917.
Davidson-Arnott, R.G.D., Law, M.N., 1990. Seasonal patterns and controls on sediment supply to coastal foredunes, Long Point, Lake Erie. In: Nordstrom, K.F., Psuty, N.P., Carter, R.W.G. (Eds.), Coastal Dunes: Form and Process. Wiley, Chichester, U. K., pp. 177–200.
Davis, P.A., 2012, Airborne digital-image data for monitoring the Colorado River corridor below Glen Canyon Dam, Arizona, 2009—Image-mosaic production and comparison with 2002 and 2005 image mosaics: U.S. Geological Survey Open-File Report 2012–1139, 82 p., http://pubs.usgs.gov/of/2012/1139/.
Davis, P.A., 2013, Natural-color and color-infrared image mosaics of the Colorado River corridor in Arizona derived from the May 2009 airborne image collection: U.S. Geological Survey Data Series 780, http://pubs.usgs.gov/ds/780/.
Durning, L.E., Sankey, J.B., Davis, P.A., Sankey, T.T., 2016a, Four-band image mosaic of the Colorado River corridor downstream of Glen Canyon Dam in Arizona, derived from the May 2013 airborne image acquisition: U.S. Geological Survey Data Series 1027, https://doi.org/10.3133/ds1027.
Durning, Laura E., Sankey Joel B., Davis, Philip A., 2016b, Four Band Image Mosaic of the Colorado River Corridor in Arizona, 2013, including Accuracy Assessment Data: U.S. Geological Survey data release, http://dx.doi.org/10.5066/F7TX3CHS.
Draut, A.E., Rubin, D.M., Dierker, J.L., Fairley, H.C., Griffiths, R.E., Hazel Jr., J.E., Yeatts, M., 2008. Application of sedimentary-structure interpretation to geoarchaeological investigations in the Colorado River Corridor, Grand Canyon, Arizona, USA. Geomorphology 101 (3), 497–509.
Draut, A. and Rubin, D., 2008. The Role of Eolian Sediment in the Preservation of Archeologic Sites Along the Colorado River Corridor in Grand Canyon National Park, Arizona, U.S. Geological Survey Professional Paper 1756, 71 p.
Draut, A.E., 2012. Effects of river regulation on aeolian landscapes, Colorado River, southwestern USA. J. Geophys. Res. Earth Surf. 117, F02022.
East, A.E., Collins, B.D., Sankey, J.B., Corbett, S.C, Fairley, H.C, Caster, J, 2016. Conditions and processes affecting sand resources at archaeological sites in the Colorado River corridor below Glen Canyon Dam, Arizona: U.S. Geological Survey Professional Paper 1825, 104 p.
Elbert, W., Weber, B., Burrows, S., Steinkamp, J., Büdel, B., Andreae, M.O., Pöschl, U., 2012. Contribution of cryptogamic covers to the global cycles of carbon and nitrogen. Nat. Geosci. 5, 459–462.
Fonstad, M.a., Dietrich, J.T., Courville, B.C., Jensen, J.L., Carbonneau, P.E., 2013. Topographic structure from motion: a new development in photogrammetric measurement. Earth Surf. Process. Land. 38 (4), 421–430. http://dx.doi.org/10.1002/esp.3366.
Fryberger, S.G., Dean, G., 1979. Dune form and wind regimes. In: McKee, E.D., (Ed.), A Study of Global Sand Seas. U.S. Geological Survey Professional Paper 1052, pp. 137–169.
Gillette, D.A., Niemeyer, T.C., Helm, P.J., 2001. Supply limited horizontal sand drift at an ephemerally crusted, unvegetated saline playa. J. Geophys. Res. Earth Surf. 106 (D16), 18085–18098. http://dx.doi.org/10.1029/2000JD900324.
Grams, P.E., Topping, D.J., Schmidt, J.C., Hazel, J.E., Kaplinski, M., 2013. Linking morphodynamic response with sediment mass balance on the Colorado River in Marble Canyon: issues of scale, geomorphic setting, and sampling design. J. Geophys. Res. Earth Surf. 118 (2), 361–381. http://dx.doi.org/10.1002/jgrf.20050.
Han, G., Zhang, G., Dong, Y., 2007. A model for the active origin and development of source-bordering dunefields on a semiarid fluvial plan: a case study from the Xiliaohe Plain, Northeast China. Geomorphology 86, 512–524. http://dx.doi.org/10.1016/j.geomorph.2006.10.010.
Harper, K.T., Belnap, J., 2001. The influence of biological soil crusts on mineral uptake by associated vascular plants. J. Arid Environ. 47, 347–357.
Hazel, J.E., Topping, D.J., Schmidt, J.C., Kaplinski, M., 2006. Influence of a dam on fine-sediment storage in a canyon river. J. Geophys. Res. Earth Surf. 111 (F1).
Hesp, P., 2002. Foredunes and blowouts: initiation, geomorphology and dynamics. Geomorphology 48, 245–268. http://dx.doi.org/10.1016/S0169-555X(02)00184-8.
Hesp, P.A., Dillenburg, S.R., Barboza, E.G., Tomazelli, L.J., Ayup-Zouain, R.N., Esteves, L.S., Gruber, N.L.S., Toldo Jr., E.E., Tabajara, L.L.C.D.A., Clerot, L.C.P., 2005. Beach ridges, foredunes or transgressive dunefields? Definitions and an examination of the Torres to Tramandai barrier system, southern Brazil. An. Acad. Bras. Cienc. 77, 493–508. http://dx.doi.org/10.1590/S0001-37652005000300010.
Houser, C., 2009. Synchronization of transport and supply in beachdune interaction. Prog. Phys. Geogr. 33, 733–746. http://dx.doi.org/10.1177/0309133309350120.
Houser, C., Mathew, S., 2011. Alongshore variation in foredune height in response to transport potential and sediment supply: South Padre Island, Texas. Geomorphology 125, 62–72. http://dx.doi.org/10.1016/j.geomorph.2010.07.028.
Ivester, A.H., Leigh, D.S., 2003. Riverine dunes on the Coastal Plain of Georgia, USA. Geomorphology 51, 289–311.
Kasprak, A., Magilligan, F.J., Nislow, K.H., Snyder, N.P., 2012. A Lidar-derived evaluation of watershed-scale large woody debris sources and recruitment mechanisms: Coastal Maine, USA. River Res. Appl. 28 (9), 1462–1476. http://dx.doi.org/10.1002/rra.1532.

Kasprak, A., Caster, J., Bangen, S.G., Sankey, J.B., 2017. Geomorphic process from topographic form: automating the interpretation of repeat survey data in river valleys. Earth Surf. Process. Landforms. http://dx.doi.org/10.1002/esp.4143.
Kasprak, A., Sankey, J.B., Buscombe, D., East, A., Grams, P.G., U.S. Geological Survey, Unpublished results. Quantifying and forecasting the response of river valley sediment connectivity to altered hydrology and land cover.
Kocurek, G., Lancaster, N., 1999. Aeolian system sediment state: theory and Mojave Desert Kelso dune field example. Sedimentology 46, 505–515. http://dx.doi.org/10.1046/j.1365-3091.1999.00227.x.
Lane, S.N., Westaway, R.M., Murray Hicks, D., 2003. Estimation of erosion and deposition volumes in a large, gravel-bed, braided river using synoptic remote sensing. Earth Surf. Process. Land. 28 (3), 249–271.
Lettau, K., Lettau, H., 1978. Experimental and micro-meteorological field studies of dune migration. In: Lettau, H.H., Lettau, K. (Eds.), Exploring the World's Driest Climate. University of Wisconsin, Madison, pp. 110–147.
Leyland, J., Hackney, C.R., Darby, S.E., Parsons, D.R., Best, J.L., Nicholas, A.P., Aalto, R., Lague, D., 2017. Extreme flood-driven fluvial bank erosion and sediment loads: direct process measurements using integrated Mobile Laser Scanning (MLS) and hydroacoustic techniques. Earth Surf. Process. Land. 42 (2), 334–346.
Liu, B., Couthard, T.J., 2015. Mapping the interactions between rivers and sand dunes: implications for fluvial and aeolian geomorphology. Geomorphology 246–257.
Lu, P., Mo, D., Wang, H., Yang, R., Tian, Y., Chen, P., Lasaponara, R., Masini, N., 2017. On the relationship between holocene geomorphic evolution of rivers and prehistoric settlements distribution in the Songshan Mountain Region of China. Sustainability 9 (1), 114.
Magirl, C.S., Breedlove, M.J., Webb, R.H., Griffiths, P.G., 2008. Modeling water-surface elevations and virtual shorelines for the Colorado River in Grand Canyon, Arizona, U. S. Geol. Surv. Sci. Invest. Rep., 2008–5075, 32 pp.
Marqués, M.A., Psuty, N.P., Rodriguez, R., 2001. Neglected effects of eolian dynamics on artificial beach nourishment: the case of Riells, Spain. J. Coastal Res. 17, 694–704.
May, J.H., 2014. Source-bordering dune. In: Encyclopedia of Planetary Landforms. doi: 10.1007/978-1-4614-9213-9_588-1.
Muhs, D.R., Roskin, J., Tsoar, H., Skipp, G., Budahn, J.R., Sneh, A., Porat, N., Stanley, J.D., Katra, I., Blumberg, D.G., 2013. Origin of the Sinai-Negev erg, Egypt and Israel: mineralogical and geochemical evidence for the importance of the Nile and sea level history. Quat. Sci. Rev. 69, 28–48.
Nilsson, C., Berggren, K., 2000. Alterations of Riparian Ecosystems Caused by River Regulation: dam operations have caused global-scale ecological changes in riparian ecosystems. How to protect river environments and human needs of rivers remains one of the most important questions of our time. Bioscience 50 (9), 783–792.
Nilsson, C., Reidy, C.A., Dynesius, M., Revenga, C., 2005. Fragmentation and flow regulation of the world's large river systems. Science 308 (5720), 405–408.
Nordstrom, K.F., Jackson, N.L., 1992. Effect of source width and tidal elevation changes on aeolian transport on an estuarine beach. Sedimentology 39, 769–778. http://dx.doi.org/10.1111/j.1365-3091.1992.tb02152.x.
Page, K.J., 1971. Riverine source bordering sand dune. Aust. Geogr. 11 (6), 603–605.
Page, K.J., Dare-Edwards, A.J., Owens, J.W., Frazier, P.S., Kellett, J., Price, D.M., 2001. TL chronology and stratigraphy of riverine source bordering sand dunes near Wagga Wagga, New South Wales, Australia. Quat. Int. 83, 187–193.
Pederson, J.L., O'Brien, G.R., 2014. Patterns in the landscape and erosion of cultural sites along the Colorado River Corridor in Grand Canyon, USA. Geoarchaeology 29 (6), 431–447.
Pearce, K.I., Walker, I.J., 2005. Frequency and magnitude biases in the 'Fryberger' model, with implications for characterizing geomorphically effective winds. Geomorphology 68, 39–55.
Psuty, N.P., 1996. Coastal foredune development and vertical displacement. Z. Geomorphol., 102 (Suppl.), 211–221.
Reheis, M.C., Budahn, J.R., Lamothe, P.J., 2002. Geochemical evidence for diversity of dust sources in the southwestern United States. Geochim. Cosmochim. Acta 66, 1569–1587. http://dx.doi.org/10.1016/S0016-7037(01)00864-X.
Rendell, H.M., Clarke, M.L., Warren, A., Chappell, A., 2003. The timing of climbing dune formation in southwestern Niger: Fluvio-aeolian interactions and the role of sand supply. Quat. Sci. Rev. 22, 1059–1065. http://dx.doi.org/10.1016/S0277-3791(03)00026-X.
Roskin, J., Katra, I., Agha, N., Porat, N., Barzilai, O., 2014. Rapid anthropogenic response to short-term local aeolian and fluvial palaeoenvironmental changes during the late pleistocene-holocene transition. Quat. Sci. Rev. 99, 176–192.
Rubin, D.M., 2012. A unifying model for planform straightness of ripples and dunes in air and water. Earth Sci. Rev. 113, 176–185.
Rubin, D.M., Hunter, R.E., 1987. Bedform alignment in directionally varying flows. Science 237 (4812), 276–278.
Rubin, D.M., Topping, D.J., Schmidt, J.C., Hazel, J., Kaplinski, M., Melis, T.S., 2002. Recent sediment studies refute Glen Canyon Dam hypothesis. Eos, Trans. Amer. Geophys. Union 83 (25), 273–278.
Sankey, J.B., Draut, A.E., 2014. Gully annealing by aeolian sediment: field and remote-sensing investigation of aeolian–hillslope–fluvial interactions, Colorado River corridor, Arizona, USA. Geomorphology 220, 68–80.
Sankey, J.B., Ralston, B.E., Grams, P.E., Schmidt, J.C., Cagney, L.E., 2015. Riparian vegetation, Colorado River, and climate: five decades of spatiotemporal dynamics in the Grand Canyon with river regulation. J. Geophys. Res. Biogeosci. 120 (8), 1532–1547.
Sankey, J.B., Kasprak, A., Caster, J.C., East, A.E., 2018. The response of source-bordering aeolian dunefields to sediment supply changes 2: controlled floods of the Colorado River in Grand Canyon, AZ, USA. Aeolian Res. 10. http://dx.doi.org/10.1016/j.aeolia.2018.02.004.
Schmidt, J.C., 1990. Recirculating flow and sedimentation in the Colorado River in Grand Canyon, Arizona. J. Geol. 98 (5), 709–724.
Schumm, S.A., 1979. Geomorphic thresholds: the concept and its applications. Trans. Inst. Br. Geographers 485–515.
Sherman, D.J., Lyons, W., 1994. Beach-state controls on aeolian sand delivery to coastal dunes. Phys. Geogr. 15, 381–395.
Simiu, E., Scanlan, R.H., 1978. Wind Effects on Structures: An Introduction to Wind Engineering. Wiley Press, New York, pp. 458.
Topping, D.J., Rubin, D.M., Vierra, L.E., 2000. Colorado River sediment transport: 1. Natural sediment supply limitation and the influence of Glen Canyon Dam. Water Resour. Res. 36 (2), 515–542.
Topping, D.J., Schmidt, J.C., Vierra, L.E., 2003. Computation and analysis of the instantaneous-discharge for the Colorado River at Lees Ferry, Arizona: May 8, 1921, through September 30, 2000 U.S. Geological Survey Professional Paper 1677, 118 p.
Vanderwal, R.L., 1978. Adaptive technology in southwest Tasmania. Austr. Archaeol. 8, 107–127.
Vericat, D., Wheaton, J.M., Brasington, J., 2017. Revisiting the Morphological Approach: Opportunities and Challenges with Repeat High-Resolution Topography, Gravel-Bed Rivers Process Disasters, 121.
Viles, H., 2012. Microbial geomorphology: a neglected link between life and landscape. Geomorphology 157–158, 6–16.
Walker, I.J., Shugar, D.H., 2013. Secondary flow deflection in the lee transverse dunes with implications for dune morphodynamics and migration. Earth Surf. Process. Land. 38, 1642–1654.
Walker, I.J., Hesp, P.A., Davidson-Arnott, R.G.D., Ollerhead, J., 2006. Topographic steering of alongshors airflow over a vegetated foredune: Greenwich Dunes, Prince Edward Island, Canada. J. Coastal Res. 22, 1278–1291.
Werner, B.T., 1995. Eolian dunes: computer simulations and attractor interpretation. Geology 23 (12), 1107–1110.
Westoby, M.J., Brasington, J., Glasser, N.F., Hambrey, M.J., Reynolds, J.M., 2012. "Structure-from-Motion" photogrammetry: a low-cost, effective tool for geoscience applications. Geomorphology 179, 300–314. http://dx.doi.org/10.1016/j.geomorph.2012.08.021.
Wheaton, J.M., Brasington, J., Darby, S.E., Sear, D.A., 2010. Accounting for uncertainty in DEMs from repeat topographic surveys: improved sediment budgets. Earth Surf. Process. Land. 35–2, 136–156.
Wheaton, J.M., Brasington, J., Darby, S.E., Kasprak, A., Sear, D., Vericat, D., 2013. Morphodynamic signatures of braiding mechanisms as expressed through change in sediment storage in a gravel-bed river. J. Geophys. Res. Earth Surf. 118 (2), 759–779. http://dx.doi.org/10.1002/jgrf.20060.
Wheaton, J.M., Fryirs, K.A., Brierley, G., Bangen, S.G., Bouwes, N., O'Brien, G., 2015. Geomorphic mapping and taxonomy of fluvial landforms. Geomorphology 248, 273–295. http://dx.doi.org/10.1016/j.geomorph.2015.07.010.
Wiggs, G.F.S., O'Hara, S.L., Wegerdt, J., Van Der Meer, J., Small, I., Hubbard, R., 2003. The dynamics and characteristics of aeolian dust in dryland Central Asia: possible impacts on human exposure and respiratory health in the Aral Sea basin. Geogr. J. 169, 142–157. http://dx.doi.org/10.1111/1475-4959.04976.
Williams, R.D., Brasington, J., Vericat, D., Hicks, D.M., 2014. Hyperscale terrain modelling of braided rivers: fusing mobile terrestrial laser scanning and optical bathymetric mapping. Earth Surf. Process. Land. 39 (2), 167–183. http://dx.doi.org/10.1002/esp.3437.
Wopfner, H., Twidale, C.R., 1988. Formation and age of desert dunes in the Lake Eyre depocenters in central Australia. Geol. Rundsch. 77, 815–834. http://dx.doi.org/10.1007/BF01830187.
Wright, S.A., Melis, T.S., Topping, D.J., Rubin, D.M., 2005. Influence of Glen Canyon Dam operations on downstream sand resources of the Colorado River in Grand Canyon. U. S. Geological Survey Circular, (1282), pp. 17-32.
Yamartino, R.J., 1984. A comparison of several "single-pass" estimators of the standard deviation of wind direction. J. Climate Appl. Meteorol. 23 (9), 1362–1366.
Yu, L., Lai, Z., An, P., 2013. OSL chronology and paleoclimatic implications of paleodunes in the middle and southwestern Qaidam Basin, Qinghai-Tibetan Plateau. Sci. Cold Arid Regions 5 (2), 211–219.